Composition-dependence of relative static permittivity in ePPC-SAFT for mixed-solvent alkali halides

Yang, Fufang; Kontogeorgis, Georgios M.; de Hemptinne, Jean-Charles

Published in:
Fluid Phase Equilibria

Link to article, DOI:
10.1016/j.fluid.2024.114103

Publication date:
2024

Document Version
Publisher's PDF, also known as Version of record

Fluid Phase Equilibria 583 (2024) 114103

Contents lists available at ScienceDirect

Fluid Phase Equilibria

journal homepage: www.journals.elsevier.com/fluid-phase-equilibria

Composition-dependence of relative static permittivity in ePPC-SAFT for mixed-solvent alkali halides

Fufang Yang [a,b], Georgios M. Kontogeorgis [b], Jean-Charles de Hemptinne [a,*]

[a] IFP Energies Nouvelles, 1 et 4 Avenue de Bois-Préau, 92852 Rueil-Malmaison Cedex, France
[b] Center for Energy Resources Engineering (CERE), Department of Chemical and Biochemical Engineering, Technical University of Denmark, 2800 Kgs Lyngby, Denmark

ARTICLE INFO

Keywords:
ePPC-SAFT
Mixed-solvent electrolyte solutions
Relative static permittivity
Mean-ionic activity coefficient
Vapor-liquid equilibria
Density

ABSTRACT

This work investigates the impact of the solvent and salt composition dependence of the relative static permittivity (RSP), a key input of the primitive electrolyte model, on the ePPC-SAFT model for mixed-solvent electrolyte solutions. Systematic deviations of mean ionic activity coefficient (MIAC) are observed as the aqueous ePPC-SAFT model is extended to mixed-solvent electrolyte solutions. To accurately represent the thermodynamic properties, approaches are proposed to correct the model's co-solvent and/or salt composition dependence without changing the aqueous part of the model: the RSP co-solvent composition dependence, the salt composition dependence in the co-solvent, or both are corrected. The obtained model is parameterized in an ion-specific approach based on critically evaluated databases of MIAC, vapor-liquid equilibria, and density. All 3 approaches accurately represent the thermodynamic properties, significantly improving upon the original RSP model. However, in an analysis of the contribution of the terms to the ionic and solvent activity coefficients, unphysical increase of the MSA contribution to MIAC is observed when only the salt composition dependence is corrected in the RSP model. Furthermore, unphysical vapor pressure elevation is predicted in the (alcohol + salt) binary mixtures when both co-solvent and salt composition dependence are corrected. Therefore, it is recommended to correct for the RSP co-solvent composition dependence only. In addition, the behavior of MIAC with alcohol composition and salt type, the effective RSP calculated using the model, and the extrapolation of the ePPC-SAFT to non-aqueous electrolyte solutions are discussed.

1. Introduction

Accurate modeling of mixed-solvent electrolyte thermodynamic properties is important in various industrial applications, such as CO_2 capture and sequestration [1], flue gas treatment [2], desalination [3], scale formation [4], corrosion resistance enhancement [5], batteries [6], pharmaceutical processes [7], etc. Although many models have been developed over the years to describe the behavior of electrolyte solutions, only a limited number of works specifically focused on mixed-solvent electrolyte solutions. The complexity of the interactions in these mixtures over wide ranges of solvent and solute compositions poses challenges for existing thermodynamic property models. As a result, the available tools are not yet well accepted or validated; the physics of the competing contributions is not yet well understood; and the best practices for property modeling still require a lot of investigation.

Table 1 shows a short summary of electrolyte statistical associating fluid theory (SAFT) and cubic plus association (CPA) works on mixed-solvent electrolyte solutions. The summary focuses on mixtures that include water, an organic solvent, and salts, i.e., works on gases, ionic liquids, or polymers are not included. The SAFT-VR+DE model [8] used the non-primitive mean spherical approximation (MSA) theory [9,10], while all the other models used the primitive MSA [11,12] or Debye--Hückel (DH) theory [13]. Maribo-Mogensen et al. [14] suggested that the primitive MSA and DH models are similar in the equation of state (EoS) framework. Most of the works included the Born term [15], with the exception of the early ePC-SAFT works [16,17]. However, in their most recent model [18,19], which was later applied on electrolyte solutions relevant to the esterification reaction [20–23], the Born term was also included. The dependence of the relative static permittivity (RSP) on temperature, density, and composition was accounted for in different ways. The RSP model presented in the SAFT-VRE [24] accounted for the ion composition dependence implicitly through the density dependence. The RSP model from Ref [24] was used in the ePPC-SAFT works [25–28] from our group. Density dependence was also accounted for in the eCPA

* Corresponding author.
E-mail address: jean-charles.de-hemptinne@ifpen.fr (J.-C. de Hemptinne).

https://doi.org/10.1016/j.fluid.2024.114103
Received 16 August 2023; Received in revised form 8 April 2024; Accepted 11 April 2024
Available online 14 April 2024

Nomenclature

Abbreviations

AAAD	Average absolute deviation
AAPD	Average absolute percentage deviation
BIP	Binary interaction parameter
DH	Debye-Hückel
ePPC-SAFT	Electrolyte polar perturbed chain statistical associating fluid theory
MIAC	Mean ionic activity coefficient
MSA	Mean spherical approximation
NAHS	Non-additive hard sphere
OC	Osmotic coefficient
OF	Objective function
RSP	Relative static permittivity
VLE	Vapor-liquid equilibria
d_T	Parameter in the Schreckenberg RSP model
d_v	Parameter in the Schreckenberg RSP model
l_{ij}	BIP for segment diameter
J	Pseudo-ionization potential
k_{ij}	BIP for dispersion energy
M	Molar mass
m	Segment number
n	Number of moles
T	Temperature
$T_{\mathrm{dep},i}$	Parameters in the temperature dependent water diameter
u_{ij}	BIP for association volume
V	Volume
w	Weight in OF
w_{ij}	BIP for association energy
x	Mole fraction
x_{p}	Dipole fraction

Greek symbols

α_{solv}	Parameter in the Simonin salt-composition dependence correction
$\gamma_{\pm}$	MIAC in mole fraction convention
$\gamma_{\pm}^{\mathrm{m}}$	MIAC in molality convention
γ_{alc}	Alcohol activity coefficient
γ_{w}	Water activity coefficient
ε	Dispersion energy
ε	Static permittivity
$\varepsilon^{\mathrm{AB}}$	Association energy
ε_{r}	Relative static permittivity
λ	Sphere softness
μ	Dipole moment
ρ	Density
σ	Segment diameter
ϕ	OC

model [29]. An advantage of including the density dependence in RSP is that, in the vapor phase, the RSP would approach 1, driving the ion composition to near-zero, avoiding the need of artificially setting this. For the short-range ion-ion and ion-solvent attractive interactions, with the exception of the ePPC-SAFT model from our group, all other mixed-solvent electrolyte models used the dispersion term. However, in the more recent works of SAFT-VRE [30] and eCPA [31,32], the association approach was also adopted, while they were not applied on mixed-solvent electrolyte solutions. In most works, the ionic diameters were regressed, making them "effective" rather than physically-based. Zhao et al. [33] suggested that, when the primitive MSA model was used, using the Pauling diameters as the ionic diameters resulted in systematic deviations of density results. In a previous work [27], we have shown that the hard sphere diameter is dominant for accurately modeling the density of the aqueous electrolyte solutions. Mixed-solvent electrolyte mean ionic activity coefficient (MIAC) was investigated in the early ePC-SAFT model [16], the SAFT-VR+DE model [8], and the eSAFT-VR Mie model [34]. In ePC-SAFT [16], a solvent-composition dependent ionic diameter had to be used. In SAFT-VR+DE [8], the focus was "to determine the predictive ability of the non-primitive model", while "a minimum number of fitted model parameters for real electrolyte solutions was used and less emphasis given to quantitative accuracy". In eSAFT-VR Mie [34,35], the salt-composition dependence of RSP was accounted for and shown to be important for the accurate representation of non-aqueous and mixed-solvent electrolyte MIAC. In all other models, mixed-solvent electrolyte MIAC was not investigated. This property is much more challenging to model compared to VLE, and is the focus of this work. The reference state of MIAC is always molality, where molality refers to the mole number of salt in 1 kg of solvent mixtures. The literature summary is focused on the key factors in mixed-solvent electrolyte solution modeling. For more detailed reviews of the electrolyte models, please refer to Ref [25,34,36–38].

In the ePPC-SAFT model, the residual Helmholtz energy is a sum of the hard-sphere, dispersion, chain, polar, association, MSA, and Born terms. The model was proposed by Rozmus et al. [44], and was revised and extended to mixed-solvent electrolyte solutions by Ahmed et al. [25] using improved water parameters [45]. Roa Pinto et al. [26] investigated the temperature-dependence of the MIAC of the aqueous NaCl solutions and the modeling approaches for the short-range ion-ion and ion-solvent attractive interactions. The Schreckenberg [24], Pottel [46], and Simonin [47] RSP models were compared. Among these, the Simonin model included adjustable parameters that accounted for the salt composition dependence. It was found that, when the adjustable RSP parameters for salt composition dependence were regressed along with the EoS parameters for the aqueous alkali halide solutions, the Simonin model RSP approached the values of the Schreckenberg model. The salt composition dependence was much weaker compared to the experimental data, agreeing with the conclusions by Maribo-Mogensen et al. [48] Furthermore, aqueous electrolyte solutions could be modeled with very high accuracy even with constant water RSP (as shown in the Supplementary Material (Tables S1 and S2)). In recent works [27,28], we have compared various modeling approaches and obtained accurate parameter sets for the aqueous alkali halide solutions based on reference databases [49,50]. Two distinct analyses were performed in the previous investigation: one was the impact of the short-range attraction term used for describing ion-ion and ion-solvent interaction (dispersion or association) and the other was related to the parameterization methodology: salt-specific or ion-specific. Regarding the description of short-range attractions, the SAFT association term was shown to be advantageous compared to using the dispersion or both the dispersion and association terms (noted as full). On the parameterization issue, the number of parameters was kept reasonable by imposing that the ionic diameters follow the same relative magnitudes as the Pauling diameters (with the exception of F^-). It shows that ion-specific parameters can provide both good results and interesting trends. We then concluded that only the association short-range attraction would be kept for future work (with the exception of Li^+), with ion-specific parameters. Based on systematic comparisons of modeling approaches, accurate parameters were published in our previous works on the aqueous alkali halide solutions.

In this work, the ePPC-SAFT model is extended to mixed-solvent electrolyte solutions. We find that the solvent and/or salt composition dependence of the model is off for the MIAC of the mixed-solvent electrolyte solutions, while VLE and density can be accurately represented as the model is extended from the previous works with no change in the modeling framework. Such distinction was not observed in our previous

works on the aqueous alkali halide solutions, regardless of the used RSP models. Although the composition dependence could be corrected in several parts of the model, we propose to correct it through the RSP. A few RSP models are presented to improve the MIAC results. All of these models reduce to the original Schreckenberg model in the aqueous solutions, making sure that there is no need to reparametrize the aqueous solutions. Thus, potentially, the approach could be used for extending other aqueous electrolyte EoSs to mixed-solvent solutions without changing the aqueous model and parameters. The manuscript proceeds as follows. In Section 2, the RSP models and the parameterization procedure are explained. In Section 3, results are shown for mixed-solvent electrolyte MIAC, VLE, and density. In Section 4, the behavior of MIAC with alcohol composition and salt type, the contributions of terms, the calculated mixed-solvent electrolyte RSP using the models, and the extrapolation to non-aqueous electrolyte solutions are analyzed. In Section 5, conclusions are presented.

2. Method

In the ePPC-SAFT model [25–28,44,45], the residual Helmholtz energy is,

$$A^{\mathrm{res}} = A^{\mathrm{hc}} + A^{\mathrm{disp}} + A^{\mathrm{assoc}} + A^{\mathrm{polar}} + A^{\mathrm{NAHS}} + A^{\mathrm{MSA}} + A^{\mathrm{Born}} \quad (1)$$

where the superscript hc denotes hard-chain, disp denotes dispersion, assoc denotes association, polar denotes multipolar as presented in Ref [51–53], NAHS denotes non-additive hard sphere as presented in Ref [54]. For details about the equations for each term and the adjustable parameters (unary and binary), please refer to Ref [25,26]. The primitive MSA model is used for the electrostatic interaction [11,12]. The Born term is included for the solvation effect [15]. In this section, the focus will be on the relative static permittivity (RSP) models and the parameterization procedure.

2.1. Relative static permittivity (RSP) models

In our previous works on the aqueous electrolyte solutions, we found that the thermodynamic properties could be modeled with high accuracy, regardless of the used RSP model. However, when we first attempted to extend the ePPC-SAFT model to mixed-solvent electrolyte solutions, large systematic deviations were observed in MIAC. In this work, 4 RSP models are compared, noted as RSP-1, −2, −3, and −4, to identify possible solutions for improving the composition dependence of ePPC-SAFT for mixed-solvent electrolyte solutions. In our accurate aqueous electrolyte parameterizations [27,28], the Schreckenberg model (RSP-1) was used. RSP-2, −3, and −4 are different from RSP-1 only when a second (non-aqueous) solvent is introduced, and reduce to RSP-1 in aqueous electrolyte solutions. Thus, there is no need to reparametrize the aqueous electrolyte solutions. Below are descriptions of the RSP models.

- RSP-1 denotes the original Schreckenberg model [24]:

Table 1
Short summary of literature electrolyte SAFT and CPA works on mixed-solvent electrolyte solutions.

	Reference	Electrostatic	Born	RSP	Short-range ion-ion and ion-solvent attractive interactions	Ionic diameters	Properties for mixed-solvent electrolyte solutions
ePC-SAFT	Held et al. 2012 [16]	DH	No	$\varepsilon_r(T, x_{\mathrm{solv}})$	Dispersion for ion-solvent, zero for ion-ion	Solvent-specific (regressed)	MIAC of (water + methanol/ethanol + salt) and (water + methanol + ethanol + salt), and density of (water + ethanol + salt)
Revised ePC-SAFT	Held et al. 2014 [17]	DH	No	$\varepsilon_r(T, x_{\mathrm{solv}})$	Dispersion for cation-anion and ion-solvent	Effective (regressed)	LLE of (water + benzene/toluene/1-butanol + salt)
SAFT-VRE	Schreckenberg et al. 2014 [24]	Primitive MSA	Yes	$\varepsilon_r(T, \rho, x_{\mathrm{solv}})$ [a]	Dispersion for ion-ion (including like-ion) and ion-solvent	Effective (regressed)	VLE of (water + methanol + salt) and LLE of (water + 1-butanol + salt)
eCPA	Maribo-Mogensen et al. 2015 [29] and Konteogeorgis et al. 2018 [37]	DH	Yes	$\varepsilon_r(T, \rho, x_{\mathrm{solv}}, x_{\mathrm{ion}})$	Huron-Vidal + NRTL mixing rule for ion-solvent, zero for ion-ion	Marcus diameters [39] for the co-volume and DH, and Born diameters from hydration free energy	SLE of (water + methanol/ethanol/ethylene glycol + salt), LLE of (water + 1-propanol + salt), and VLE of (water + methanol + salt)
SAFT-VR+DE	Das et al. 2018 [8]	Non-primitive MSA	NA [b]	NA [b]	Dispersion for ion-ion (including like-ion) and ion-solvent	Ionic diameters from a few sources [40–42]	MIAC of (water + methanol/ethanol + salt)
ePPC-SAFT	Ahmed et al. 2018 [25]	Primitive MSA	Yes	$\varepsilon_r(T, \rho, x_{\mathrm{solv}}, x_{\mathrm{ion}})$	Association for cation-anion and ion-solvent	Pauling diameters [43] for hard-sphere and Born, effective (regressed) for MSA	VLE of (water + methanol/ethanol + salt)
"advanced" ePC-SAFT	Ascani et al. 2021 [18, 19,23]	DH	Yes	$\varepsilon_r(x_{\mathrm{solv}}, x_{\mathrm{ion}})$	Dispersion for ion-ion (including like-ion) and ion-solvent	Effective (regressed)	LLE of (water + 1-butanol/1-pentanol/MEK/MIBK + salt) and (water + 1-propanol/1-butanol + salt + salt), partition coefficient and pH of (water + toluene + carboxylic acid)
eSAFT-VR Mie	Novak et al. 2023 [34]	DH	Yes	$\varepsilon_r(T, x_{\mathrm{solv}}, x_{\mathrm{ion}})$	Dispersion for ion-solvent, zero for ion-ion	Effective (regressed)	VLE and MIAC of (water + methanol/ethanol + salt), and LLE of (water + 1-propanol/1-butanol + salt)
ePPC-SAFT	This work	MSA	Yes	$\varepsilon_r(T, \rho, x_{\mathrm{solv}}, x_{\mathrm{ion}})$	Association for cation-anion and ion-solvent	Effective (regressed) diameters for hard-sphere and MSA, and Born diameters from Gibbs energy of solvation	VLE, MIAC, and density of (water + methanol/ethanol + salt)

Note:
[a] The RSP model is implicitly dependent on x_{ion} through ρ.
[b] NA = not applicable: non-primitive MSA does not require a Born term, neither a RSP model as inputs. It actually computes them from first principles.

$$\varepsilon_r = 1 + \frac{n_{solv}}{V} d_v \left(\frac{d_T}{T} - 1 \right) \quad (1a)$$

where ε_r is the RSP, n_{solv} is the number of moles of the solvent, V is the total volume, d_v and d_T are parameters determined using the mixing rules:

$$d_v = \frac{\sum_{solv} n_i d_{v,i}}{\sum_{solv} n_i} \quad (2a)$$

$$d_T = \frac{\sum_{solv} n_i d_{T,i}}{\sum_{solv} n_i} \quad (2b)$$

- RSP-2 denotes the Schreckenberg model with effective alcohol RSP. The model is still of Schreckenberg (Eq. (1)), except that the alcohol d_v and d_T parameters are regressed along with the alcohol-ion binary interaction parameters (BIPs) for reference mixtures (as will be discussed later). In this way, the RSP alcohol composition dependence is modified without changing the equations nor the parameters for (water + salt). The modification is introduced because of the difficulties encountered with RSP-1 for representing MIAC at high alcohol composition. A shortcoming of RSP-2 is that the experimental RSP of the salt-free solvent mixture is not correctly represented. However, one can argue that: 1) RSP is input rather than output of the electrolyte SAFT model with primitive MSA; 2) mixed-solvents form different solvation structures around ions compared to pure water [55,56], and the distinctive behavior is not guaranteed to be correctly accounted for in the model that has been developed and parameterized on the aqueous electrolyte solutions. In RSP-1 and −2, salt composition dependence is accounted for implicitly through the density dependence, and thus is not reflected in the salt composition derivative.
- RSP-3 denotes the revised Simonin model with different salt composition dependence for water and for the co-solvent. The model explicitly accounts for the salt composition dependence of the RSP, and is based on the empirical aqueous electrolyte solution RSP model proposed by Simonin et al. [47]:

$$\varepsilon_r = \frac{\varepsilon_{r,0}}{1 + \sum_{solv} \alpha_{solv} x^0_{solv} \sum_{ion} x_{ion}} \quad (3)$$

where ε_0 is calculated using the Schreckenberg model (RSP-1). Remember that this value depends on volume which is affected by the presence of salts. The new parameter, α_{solv}, accounts for a more explicit correction for the salt composition dependence of RSP. Its impact is proportional to the salt free mole fraction of the solvent, x^0_{solv}; whereas x_{ion} is the mole fraction of the ion. Using $\alpha_{water} = 0$ ensures that the model reduces to RSP-1, i.e., same as in our previous works for the aqueous electrolyte solutions. The alcohol α_{solv} parameter is regressed along with the alcohol-ion BIPs for reference mixtures (as will be discussed later). In this way, the RSP salt composition dependence in water and in the co-solvent is accounted for distinctively.

- RSP-4: Both co-solvent and salt composition dependence are corrected by combining the treatments in RSP-2 and −3. RSP-2 is used as $\varepsilon_{r,0}$ in Eq. (3). Thus, the alcohol d_v, d_T, and α_{solv} parameters are regressed along with the alcohol-ion BIPs for reference mixtures (as will be discussed later).

Table 2 shows a schematic of the relationship between the RSP models.

2.2. Objective function, reference database, and parameterization

Table 3 shows the parameters of the solvents in ePPC-SAFT. The water parameters, methanol parameters and methanol-water BIPs were obtained in our previous works [25,45,58]. The pure ethanol parameters are regressed to experimental vapor pressure, saturated liquid density, and saturated vapor density data between 273.16 K and 463.24 K calculated using the empirical correlations [59]. The average absolute percentage deviations (AAPDs) are 0.13% for vapor pressure, 0.11% for saturated liquid density, and 0.13% for saturated vapor density. The ethanol-water BIPs are obtained using experimental binary VLE data [60–72] between 298.15 K and 372.45 K. The AAPD for VLE pressure is 0.73%. The average absolute absolute deviation (AAAD) for vapor phase mole fraction is 0.0068. The parameters are regressed using the evolutionary algorithm [73], which is helpful for avoiding local minima. The definitions of AAPD and AAAD are:

$$\text{AAPD} = \frac{1}{n_{dp}} \sum_{i}^{n_{dp}} \left| \frac{X_i^{cal} - X_i^{exp}}{X_i^{exp}} \right| \quad (4a)$$

$$\text{AAAD} = \frac{1}{n_{dp}} \sum_{i}^{n_{dp}} \left| X_i^{cal} - X_i^{exp} \right| \quad (4b)$$

Table 2
Schematic of the relationship between the RSP models.

	Schreckenberg model [24] (Eq. (1)) without salt-composition correction	Schreckenberg model (Eq. (1)) with Simonin correction [47] for the alcohol-salt pair (Eq. (3)), adding a new adjustable parameter, α_{solv}.
Original alcohol d_v and d_T parameters (from Ref [24])	RSP-1	RSP-3
Effective alcohol RSP by refitting alcohol d_v and d_T parameters	RSP-2	RSP-4

Table 3
Parameters of the solvents in ePPC-SAFT. For details about the equations for each term and the adjustable parameters (unary and binary), please refer to Ref [25,26]. The binary interaction parameters (BIP) are with water.

Parameter	Water [a]	Methanol [b]	Ethanol
Segment number, m	1.02122	2.827	3.041
Segment diameter, σ(Å)	2.2423	2.632	2.925
$T_{dep,1}$(Å)	0.51212	–	–
$T_{dep,2}$ (K^{-1})	0.001126	–	–
$T_{dep,3}$(Å·K^2)	9904.13	–	–
Dispersion energy, ε/k_B (K)	201.747	166.8	170.2
Association energy, ε^{AB}/k_B (K)	1813	2069.09	2087.5
Association volume, κ^{AB}	0.044394	0.2373	0.05441
Association type	4C	2B	3B
Sphere softness, λ	0.203	0.12	0.12
Dipole moment, μ (D)	1.85	1.7	1.83
Dipole fraction, x_p	0.276	0.35	0.5
BIP, k_{ij} [c]	–	0.00212	−0.05290
BIP, l_{ij} [c]	–	0.0178	0
BIP, w_{ij} [c]	–	−0.0352	0.05602
BIP, u_{ij} [c]	–	0.0025	0

Note:

[a] The water parameters were obtained in our previous work [45], $\sigma_w = \sigma + T_{dep,1}\exp(T_{dep,2}T) + \frac{T_{dep,3}}{T^2}$.

[b] The methanol parameters and methanol-water BIPs were obtained in our previous work [25]. The k_{ij} for methanol-water was predicted using $1 - k_{ij} = \frac{2\sqrt{J_i J_j}}{J_i + J_j}$, where J is the pseudo-ionization potential [74].

[c] The BIPs are used in the combining rules: $\varepsilon_{ij} = (1 - k_{ij})\sqrt{\varepsilon_i \varepsilon_j}$, $\sigma_{ij} = (1 - l_{ij})\frac{\sigma_i + \sigma_j}{2}$, $\varepsilon^{AB}_{ij} = (1 - w_{ij})\frac{\varepsilon^{AB}_i + \varepsilon^{AB}_j}{2}$, and $\kappa^{AB}_{ij} = (1 - u_{ij})\sqrt{\kappa^{AB}_i \kappa^{AB}_j}$.

where X denotes the properties, and n_{dp} is the number of data points for the property.

Fig. 1 shows the VLE for (water + methanol) and (water + ethanol).

For determining the alcohol-ion BIPs (and the RSP parameters in the relevant cases), the objective function includes MIAC, VLE, and density of the mixed-solvent electrolyte solutions.

$$\mathrm{OF} = \frac{\sum_{i=1}^{n_{dp}^{\gamma^\pm}} \left(\frac{\gamma^\pm_{cal} - \gamma^\pm_{exp}}{\gamma^\pm_{exp}} \right)^2}{n_{dp}^{\gamma^\pm}} + \frac{\sum_{i=1}^{n_{dp}^{p}} \left(\frac{p_{cal} - p_{exp}}{p_{exp}} \right)^2}{n_{dp}^{p}} + \frac{w \sum_{i=1}^{n_{dp}^{y}} \left(y_{cal} - y_{exp} \right)^2}{n_{dp}^{y}} + \frac{\sum_{i=1}^{n_{dp}^{\rho}} \left(\frac{\rho_{cal} - \rho_{exp}}{\rho_{exp}} \right)^2}{n_{dp}^{\rho}} \quad (5)$$

where $\gamma^\pm$ is the MIAC, p is the pressure, y is the mole fraction of the alcohol in the vapor phase, ρ is the density, n_{dp} is the number of data points for the property, and w is the weight applied only for y, because it is in absolute deviation. The default values (0.1 ~ 0.2) in ATOUT [78] are used for w after normalization.

Table 4 shows a summary of the mixed-solvent electrolyte properties (MIAC, VLE, and density) included in the parameterization. The MIAC and VLE data used in the regression have been described in detail in our previous work [49] in which the experimental datasets were evaluated. Only the datasets that were marked as R (Recommended) and T (Tentative) [79–102] in the data evaluation work are used here. The used MIAC and VLE datasets are as summarized in Ref [49]. The density data [103–115] are evaluated in this work using the support vector regression procedure as described in our previous work [50] on the reference density database for aqueous electrolyte solutions. However, as data are not as extensively available compared to the aqueous solutions, the verifications are less strict. A short summary of the density data is provided in the Supplementary Material (Table S3). The used density datasets are also provided in the Supplementary Material.

The pseudo-unary parameters for the ions and the ion-water BIPs were obtained in our previous works based on the aqueous electrolyte solutions [27,28]. The alcohol-ion BIPs (and the RSP parameters of RSP-2, −3, and −4) are obtained from minimizing Eq. (5). Table 5 shows the ion-specific parameterization procedure for the mixed-solvent electrolyte solutions. For all ions except for Li^+, w_{ij} is the only adjusted BIP. For Li^+, both w_{ij} and k_{ij} are adjusted (see Table 5). For RSP-1, for each solvent mixture, the alcohol-Na^+, alcohol-K^+, and alcohol-Cl^- BIPs are first regressed based on data of (water + alcohol + NaCl) and (water + alcohol + KCl). For RSP-2, the effective alcohol d_v and d_T parameters are regressed along with the BIPs for the 2 mixtures. Similarly, for RSP-3, the alcohol α_{solv} parameter is regressed along with the BIPs, while for RSP-4, d_v, d_T, and α_{solv} are regressed along with the BIPs, respectively for the 2 mixtures. Then, these parameters are kept the same as other alcohol-ion BIPs are regressed based on data of other (water + alcohol + salt) systems, e.g., for the RSP-2 case of (water + alcohol + NaBr), the effective alcohol d_v and d_T parameters, and the alcohol-Na^+ BIP are kept the same, while only the alcohol-Br^- BIP is regressed. In this way, the parameters are obtained in an ion-specific manner step-by-step. Whenever 2 or more parameters are regressed, the evolutionary algorithm is used. Table 6 shows the RSP parameters. Table 7 shows the alcohol-ion BIPs.

Table 4
Summary of the mixed-solvent electrolyte properties (MIAC, VLE, and density) included in the parameterization.

Water + methanol +				
	F^-	Cl^-	Br^-	I^-
Li^+		MIAC & VLE & density		
Na^+	MIAC	MIAC & VLE & density	VLE & density	
K^+		MIAC & VLE & density		
Rb^+		MIAC		
Cs^+				
Water + ethanol +				
	F^-	Cl^-	Br^-	I^-
Li^+				
Na^+	MIAC	MIAC & VLE & density		VLE & density
K^+		MIAC & VLE & density	VLE & density	VLE & density
Rb^+				
Cs^+		MIAC & density		

3. Results

3.1. MIAC

Fig. 2 shows comparisons of the MIAC of (water + methanol + NaCl) calculated using the ePPC-SAFT with the 4 RSP models at 298.15 K and 0.1 MPa and experimental data. Literature of the experimental data is as listed and explained in Section 2.2 and Ref [49]. The graphs are plotted in logarithm scale to visualize the high alcohol composition part more clearly. For easier comparisons, graphs are provided in the linear scale in the Supplementary Material (Figure S1). The percentage values noted for the curves and symbols are the salt-free weight fractions of the alcohol. The (water + NaCl) binary data and calculations are also plotted in the graphs. Compared to RSP-1, all 3 approaches present significant improvement. For the 20% salt-free alcohol weight fraction, RSP-2 does not improve very much for the deviations at high salt composition, because the alcohol composition is small and therefore the

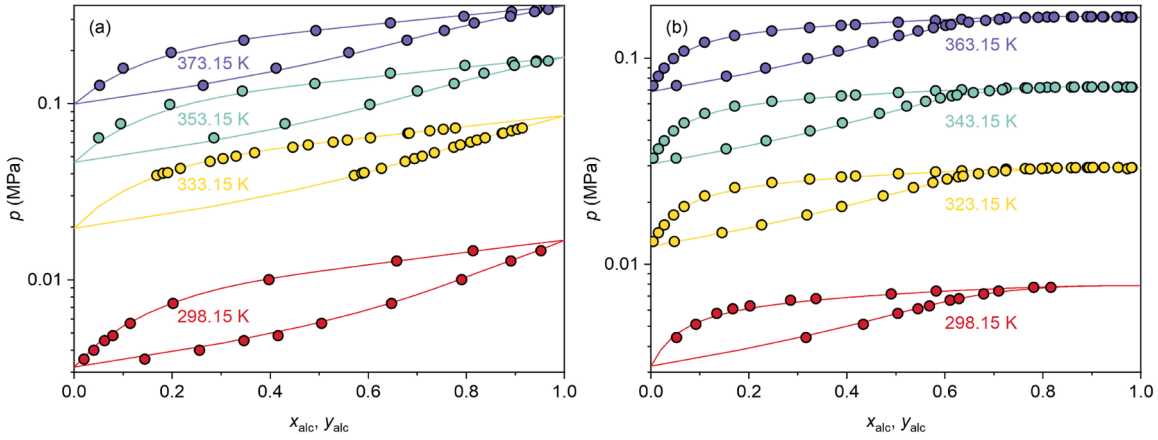

Fig. 1. VLE for (a) (water + methanol) and (b) (water + ethanol). The lines are calculated using ePPC-SAFT (PPC-SAFT here as there is no electrolyte). The symbols are experimental data [60,61,75–77].

Table 5
Ion-specific parameterization procedure of the ePPC-SAFT model for the mixed-solvent electrolyte solutions.

Order	Data	Pseudo-unary		BIPs		
		RSP-1	RSP-2	RSP-3	RSP-4	
	Water + methanol +					
1	NaCl; KCl	–	d_v & d_T	α_{solv}	d_v & d_T & α_{solv}	$w_{Na^+-methanol}$ & $w_{K^+-methanol}$ & $w_{Cl^--methanol}$
2a	NaF					$w_{F^--methanol}$
2b	NaBr					$w_{Br^--methanol}$
2c	LiCl					$w_{Li^+-methanol}$ & $k_{Li^+-methanol}$
2d	RbCl					$w_{Rb^+-methanol}$
	Water + ethanol +					
1	NaCl; KCl	–	d_v & d_T	α_{solv}	d_v & d_T & α_{solv}	$w_{Na^+-ethanol}$ & $w_{K^+-ethanol}$ & $w_{Cl^--ethanol}$
2a	NaF					$w_{F^--ethanol}$
2b	NaI; KI					$w_{I^--ethanol}$
2c	CsCl					$w_{Cs^+-ethanol}$
2d	KBr					$w_{Br^--ethanol}$

correction is not very pronounced; RSP-3 is the most accurate, because the corrections are the most pronounced at high salt composition; RSP-4 is in between RSP-2 and RSP-3. However, at higher alcohol compositions, RSP-2 and RSP-4 are more accurate than RSP-3, because the alcohol-composition corrections are more pronounced in that range. The corrections of RSP-3 focus on the salt composition dependence, and salt content is small at high alcohol content, which results in a small improvement in that same range. This problem of RSP-3 could not be visualized clearly in the linear scale graph provided in the Supplementary Material. Furthermore, this low-alcohol-composition shortcoming of RSP-2 is a special case, as will be shown later for results of the same mixture at higher temperatures. Overall, for this first case, the corrections are working as expected. Based on the first results, we prefer RSP-2 and RSP-4 over RSP-3.

MIAC data are available for (water + methanol + NaCl) at elevated temperatures. Fig. 3 shows comparisons of calculations using the ePPC-SAFT with RSP-2 and −4 at 308.15 K and 318.15 K and 0.1 MPa and experimental data. For brevity, only RSP-2 and −4 are shown. Literature of the experimental data is as listed and explained in Section 2.2 and Ref [49]. The graphs are plotted in logarithm scale to visualize the high alcohol composition results more clearly. For easier comparisons, graphs are provided in the linear scale in the Supplementary Material (Figure S2). Both models are accurate at elevated temperatures.

3.2. VLE

Figs. 4 and 5 show the comparisons of the VLE (pseudo-binary plot) of 5 mixtures calculated using the ePPC-SAFT with RSP-2 and −4 at 298.15 K and experimental data. The ternary results are plotted in pseudo-binary plots for clearer visualization, especially for the departure of the electrolyte solutions from the solvent mixtures. Both models are quite accurate for representing the experimental data. Yet the extrapolation yields sometimes unexpected results: an azeotropic behavior is generally identified by the fact that the bubble curve shows a maximum, e.g., (water + methanol + 4 M NaBr), (water + ethanol + 1 M NaCl), (water + ethanol + 1 M KCl), yet, here the dew lines always remain on the right hand side of the bubble lines, resulting in the crossing of dew lines and bubble lines, and pointing to the fact that there is no volatility inversion (alcohol always remains more volatile than water). This is observed because the liquid contains salts, while the vapor does not. The phenomena cannot be verified using experimental data, because the salt composition exceeds the solubility at high alcohol composition, at which the crossing occurs. However, the crossing is not observed in the ePPC-SAFT with RSP-4. This is because of the different salt composition dependence in the co-solvent of the RSP models. On the other hand, the ePPC-SAFT with RSP-4 predicts vapor pressure elevation for the (water + ethanol + salt) cases in the pure ethanol end, which is likely to be unphysical. The behavior is not observed in RSP-4 for (water + methanol + salt) and in RSP-2 for both (water + methanol + salt) and (water + ethanol + salt). For mixed-solvent electrolyte solutions, vapor pressure elevation occurs in cases where the salting out of one of the solvent components outweighs the salting in of the other, e.g., for (water + methanol + NaCl) [88]. However, this is not likely to happen for salt in a pure solvent. No experimental vapor pressure data was found in our literature search for the (ethanol + NaCl) and (ethanol + KCl) binaries, while experimental works reported vapor pressure depression for (methanol + NaCl) [116,117] and (ethanol + NaI) [118], which agreed with the common sense, i.e., vapor pressure depression. We therefore conclude that RSP-4 provides unphysical results, even though in this case at salt compositions that exceed the solubility limit at high alcohol composition. In summary, both RSP-2 and −4 (indeed also −1 and −3) accurately represents the VLE of mixed-solvent electrolyte solutions, while extrapolations beyond the salt solubility limits suggests preference of RSP-2 over RSP-4.

Finally, density of the mixtures solvent electrolyte solutions is also accurately represented. Table 8 shows the overall average deviations for MIAC, VLE, and density calculated using the ePPC-SAFT model with the 4 RSP models. Average and maximum deviations for each mixed-solvent electrolyte solution are provided in the Supplementary Material (Table S4), along with deviations plotted against T, x_{alc}, and x_{ion} (Figures S4-S31). The behavior of RSP-1 is similar in all cases: systematic deviations are present as salt and alcohol compositions increase.

Table 6
RSP parameters of the ePPC-SAFT model for mixed-solvent electrolyte solutions. The preset (not regressed) parameters are marked as bold and italic.

Parameter	Water	Methanol				Ethanol			
		RSP-1	RSP-2	RSP-3	RSP-4	RSP-1	RSP-2	RSP-3	RSP-4
d_v (dm^3/mol)	***0.3777*** [a]	***0.5484*** [a]	0.3106	***0.5484*** [a]	0.4027	***0.9480*** [a]	0.3033	***0.9480*** [a]	0.4008
d_T (K)	***1403*** [a]	***1011*** [a]	1296	***1011*** [a]	1114	***732.1*** [a]	1264	***732.1*** [a]	1257
α_{solv}	–	–	–	−3.885	−1.208	–	–	−5.556	−4.411

Note:
[a] The parameters are from Ref [24].

Table 7
Alcohol-ion BIPs of the ePPC-SAFT model for mixed-solvent electrolyte solutions.

BIP	Methanol				Ethanol			
	RSP-1	RSP-2	RSP-3	RSP-4	RSP-1	RSP-2	RSP-3	RSP-4
$w_{Na^+-alcohol}$	−0.03249	−0.09275	−0.06496	−0.07688	0.1342	0.1031	0.2055	0.1448
$w_{K^+-alcohol}$	0.09959	0.02891	0.08947	0.09560	0.1764	0.1644	0.2741	0.1739
$w_{Cl^--alcohol}$	0.03422	0.03542	0.1633	0.04701	0.1046	0.08255	0.1744	0.1628
$w_{F^--alcohol}$	0.3074	1.000	0.2406	0.1598	1.000	1.000	1.000	1.000
$w_{Br^--alcohol}$	−0.06330	−0.03442	0.02300	−0.02920	−0.1137	−0.2225	−0.06160	−0.1009
$w_{I^--alcohol}$					−0.1617	−0.2434	−0.1573	−0.1717
$w_{Rb^+-alcohol}$	0.07990	0.07990	0.07990	0.07990				
$w_{Cs^+-alcohol}$					0.1120	0.1099	0.1121	0.1121
$w_{Li^+-alcohol}$	−0.02615	−0.07626	0.05408	−0.3573				
$k_{Li^+-alcohol}$	−0.5580	−0.6731	−0.1971	−0.1344				

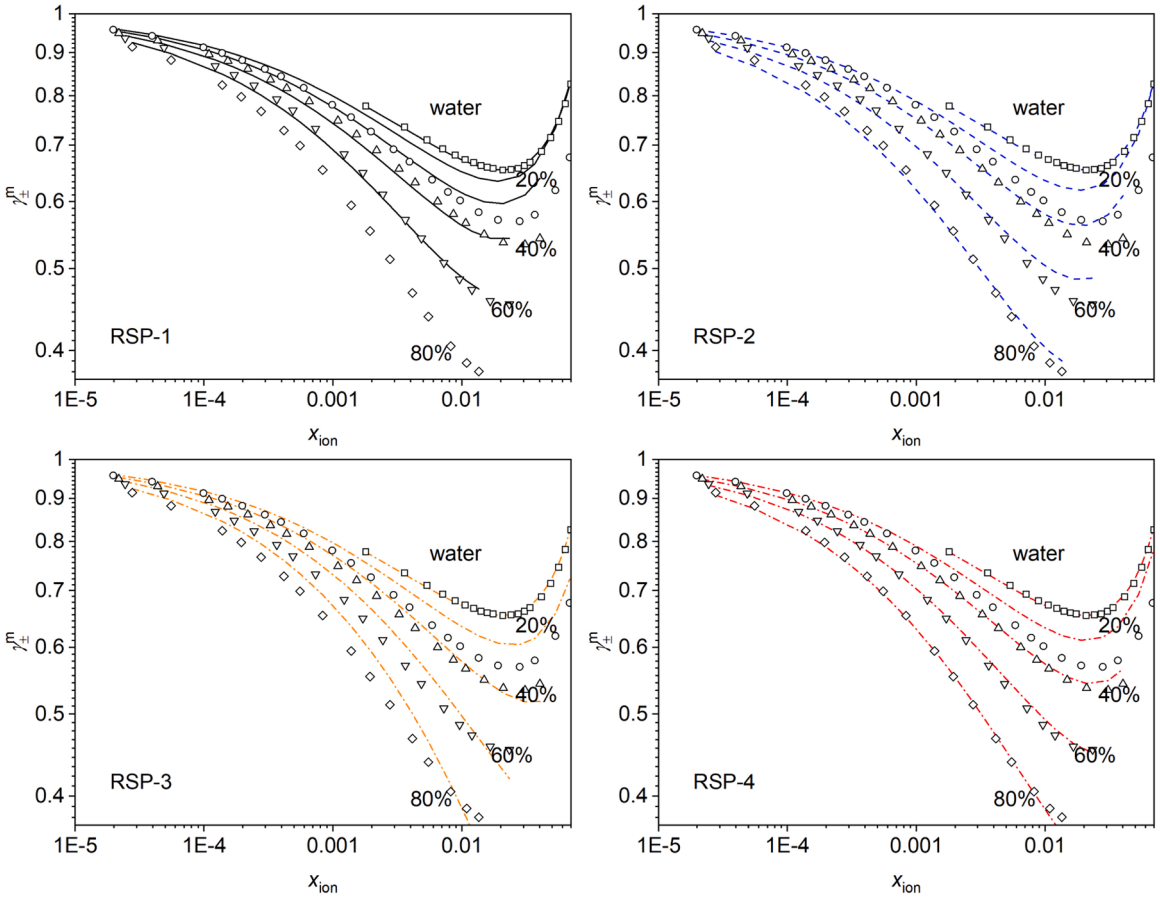

Fig. 2. Comparisons of the MIAC of (water + methanol + NaCl) calculated using the ePPC-SAFT with the 4 RSP models (lines) at 298.15 K and 0.1 MPa and experimental data (symbols). The percentage values noted for the curves and symbols are the salt-free weight fractions of the alcohol. Literature of the experimental data is as listed and explained in Section 2.2 and Ref [49]. $x_{i,\text{ion}} = \frac{n_{i,\text{ion}}}{\sum_k n_{k,\text{ion}} + \sum_k n_{k,\text{solvent}}}$ is the ion-based mole fraction of the ions, where n is the mole number. Here, all salts are monovalent. Thus, $x_{\text{cation}} = x_{\text{anion}}$ and is represented as x_{ion}.

To sum up, the ePPC-SAFT model with the alcohol and/or salt composition corrected RSP models significantly improves the modeling accuracy for the MIAC of the mixed-solvent electrolyte solutions, while maintaining the modeling accuracy for VLE and density in the range where experimental data exist; RSP-2 is our preferred model.

4. Discussion

In this section, the behavior of MIAC with alcohol composition and salt type is analyzed; the contributions of the terms to the MIAC and solvent activity coefficients are analyzed; the RSP models, which serve as intermediate functions in the electrolyte SAFT model, are discussed; extrapolation results for non-aqueous electrolyte solutions are presented.

4.1. Behavior of MIAC with alcohol composition and salt type

Fig. 6 shows the comparisons of the MIAC of 8 (water + alcohol + salt) mixtures calculated using the ePPC-SAFT with RSP-2 at 298.15 K and 0.1 MPa and experimental data. The graphs are plotted using a logarithmic scale to visualize the high alcohol composition results more clearly. The corresponding plots calculated using the ePPC-SAFT with RSP-4 are provided in the Supplementary Material (Figure S3). Literature of the experimental data is as listed and explained in Section 2.2 and

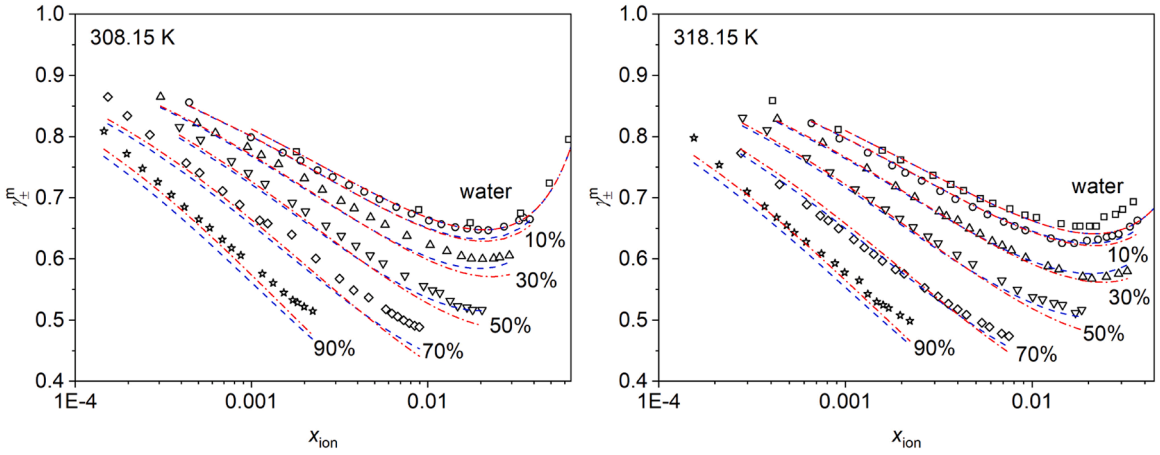

Fig. 3. Comparison of the MIAC of (water + methanol + NaCl) calculated using the ePPC-SAFT with RSP-2 (blue dashed lines) and RSP-4 (red dash-dotted lines) at 308.15 K and 318.15 K and 0.1 MPa and experimental data (symbols). The percentages in the graphs are salt-free weight fraction of the alcohol. Literature of the experimental data is as listed and explained in Section 2.2 and Ref [49].

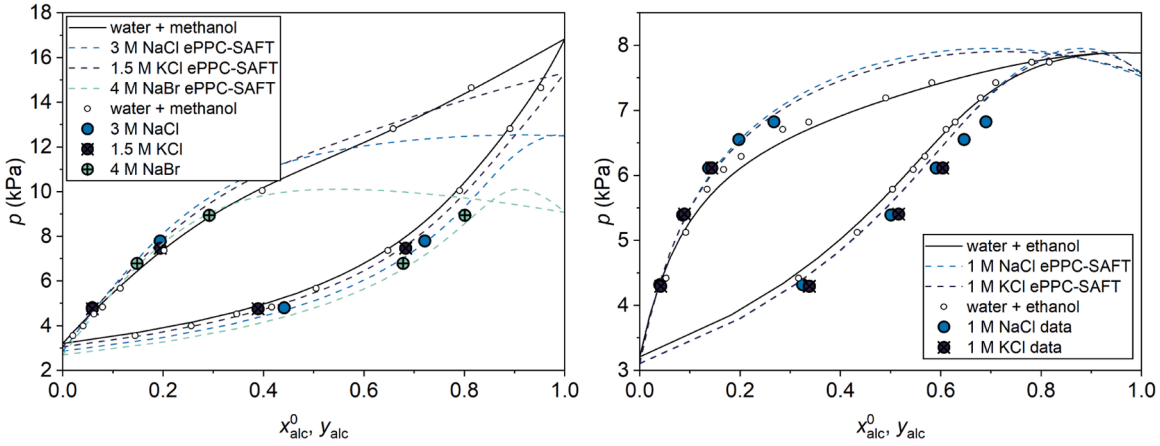

Fig. 4. Comparisons of the VLE (pseudo-binary plot) of (water + methanol + NaCl), (water + methanol + KCl), (water + methanol + NaBr), (water + ethanol + NaCl), and (water + ethanol + KCl) calculated using the ePPC-SAFT with RSP-2 at 298.15 K and experimental data. The VLE calculations of (water + alcohol) are also plotted. The experimental data of the solvent mixtures without salts are plotted in smaller symbols.

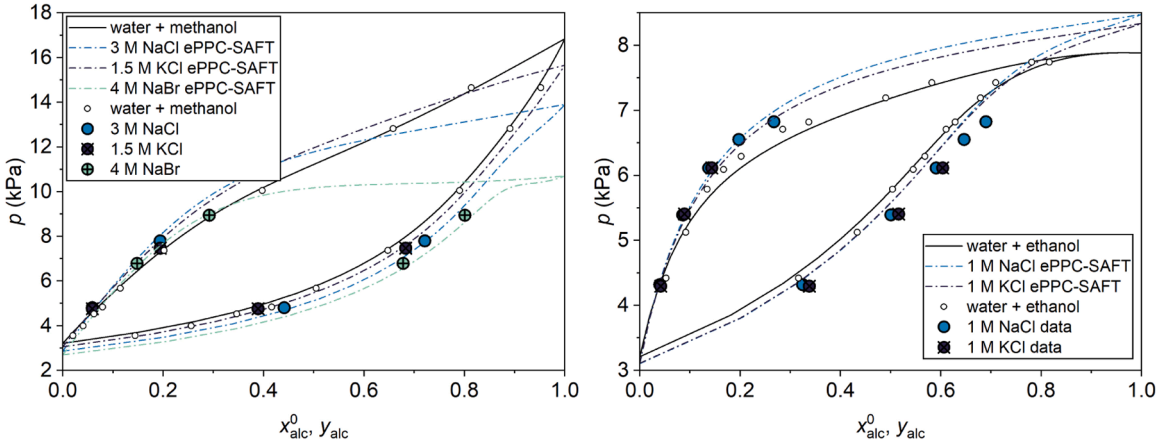

Fig. 5. Comparisons of the VLE (pseudo-binary plot) of (water + methanol + NaCl), (water + methanol + KCl), (water + methanol + NaBr), (water + ethanol + NaCl), and (water + ethanol + KCl) calculated using the ePPC-SAFT with RSP-4 at 298.15 K and experimental data. The VLE calculations of (water + alcohol) are also plotted. The experimental data of the solvent mixtures without salts are plotted in smaller symbols.

Table 8
Overall deviations of MIAC, VLE, and density calculated using the ePPC-SAFT model with the 4 RSP models. The MIAC, VLE p, and density deviations are AAPDs (Eq. (4a)). The VLE y (vapor phase composition) deviations are AAADs (Eq. (4b)).

100AAPDs (100AAADs)	MIAC	VLE p	VLE y	Density
RSP-1	11	2.5	1.8	1.3
RSP-2	4.2	2.7	1.7	1.3
RSP-3	6.9	2.8	1.8	1.3
RSP-4	3.3	2.5	1.7	1.3

Ref [49]. Notice that only a few salts are documented, which is unfortunate considering the information that such data can provide on the underlying physical phenomena (see Ref [119] for pure water). At first, it is of interest to note the composition range, limited by the salt solubility at increased alcohol composition. In this low composition range, the MIAC always decreases with salinity. Furthermore, the MIAC in mixed-solvents is always smaller than in pure water.

In general, both RSP-2 and −4 accurately represent the mixed-solvent electrolyte MIAC. Calculations using these 2 RSP models are quite close for most mixtures. However, MIAC calculated using RSP-2, compared to using RSP-4, increase more strongly with salt composition for (water + methanol + LiCl), (water + ethanol + NaCl), and (water + ethanol + CsCl): RSP-2 deviations are larger for (water + methanol + LiCl) and (water + ethanol + CsCl), and are smaller for (water + ethanol + NaCl). For (water + methanol + LiCl), both RSP-2 and −4 overestimate the MIAC at high salt composition and low alcohol composition (20% salt-free alcohol weight fraction), but are both quite accurate at 80% salt-free alcohol weight fraction. Note that the model is accurate for (water + LiCl). For (water + methanol + NaF), the experimental MIAC values at 10% salt-free alcohol weight fraction are larger than the experimental (water + NaF) MIAC values pointing to a problem in the data. Note that the (water + NaF) MIAC datasets were verified using different experimental sources in our data analysis [49]. Because MIAC in mixed-solvents is always smaller than in pure water, the data situation suggests that the mixed-solvent electrolyte MIAC dataset presents systematic deviations. However, the data inconsistency is within a few percent. In addition, the data inconsistency between the experimental MIAC data of (water + methanol + NaF) and (methanol + NaF) will be discussed in Section 4.4.

4.2. Contributions of the terms

Fig. 7 shows the contribution to the logarithm of the rational (mole fraction based) activity coefficients of the 3 compounds, salt ($\ln\gamma_{\pm}$), water ($\ln\gamma_{w}$), and alcohol ($\ln\gamma_{alc}$) of the terms (hard-chain, dispersion, association, multipolar, NAHS, MSA, and Born) of ePPC-SAFT combined with RSP-2 for (water + methanol + NaCl) at 298.15 K and 0.1 MPa. The plots for the other 3 RSP models are provided in the Supplementary Material. The activity coefficients are based on a reference state at the corresponding salt-free solvent compositions. The hard-chain, dispersion, and multipolar terms are combined and noted as "others" for clearer visualization. All 4 RSP models present the same results at 0% methanol composition. The contributions are plotted up to $x_{ion} = 0.05$ for all methanol compositions, which exceeds the solubility of NaCl at high methanol composition, as NaCl solubility decreases with increasing methanol composition. Thus, the high x_{ion} part of the high alcohol composition plots are only for observing the trends theoretically.

For $\ln\gamma_{\pm}$, the Born term changes very little with alcohol composition for RSP-1 and −2, but changes very much with alcohol composition for RSP-3 and −4. The correction of alcohol composition dependence has a marginal impact on the Born contribution to MIAC, while the correction of salt composition dependence has a significant impact. The MSA contribution is negative for all 4 RSP models. The MSA contribution decreases with both salt and alcohol compositions for RSP-1 and −2, with the latter decreasing more drastically. The correction of the alcohol composition dependence has a significant impact on the MSA contribution, whose slope at the origin is directly related to the solvent RSP. The MSA contribution of RSP-3 is not monotonic with salt composition at high alcohol composition. The behavior is not observed in the other RSP models, and is likely to be unphysical: the electrostatic contribution should decrease with increasing salt composition. A similar trend is observed in RSP-4, but not to the same extent: at 80% and 100% salt-free alcohol mole fraction, the MSA contribution changes with salt composition very slightly. However, these ranges are extrapolations, because the salt composition exceeds the solubility limit at high alcohol composition. The association contribution combines the effect of ion pairing and that of solvation. It is always positive and increases with salt and alcohol compositions, except for RSP-3. The association contributions of RSP-1, −2, and −4 are similar, with RSP-2 and −4 changing with alcohol composition slightly more strongly than RSP-1. However, for RSP-3, the association contribution is smaller at 100% alcohol composition than at 80%. The behavior is difficult to explain, and seems to be another reason to prefer RSP-2 and −4 over RSP-3. The changes of the other terms combined are similar for all 4 RSP models.

The water activity coefficient, defined as the ratio of the fugacity coefficient in the electrolyte solution divided by that in the solvent mixture without salt, is always negative, pointing to the salting-in effect of the salts for water. Split into the 4 major contributions (2 electrostatic long-range and 2 short-range), it appears that, in all 4 models, MSA is positive and Born is negative, of comparable magnitudes, and that association is negative while the other contributions, of which dispersion is the largest, are positive, also of comparable magnitudes. The net negative effect is because Born and association are slightly larger in magnitudes than their counterparts. Analyzing the trends in each of the 4 models, one may state that the correction of RSP alcohol composition dependence (RSP-2) strongly increases the alcohol composition dependence of the MSA and Born contributions, yet keeping the sum relatively constant. However, the MSA and Born contributions behave differently for RSP-3, with a non-monotonic behavior as a function of salt composition.

The methanol activity coefficient (ratio of methanol fugacity coefficient in the mixture to that in solvent mixture without salt) shows a positive trend. This points to the salting-out phenomenon that is well-known for organic compounds in salt solutions. Yet, this salting-out effect diminishes with increasing alcohol content and may actually become salting-in for some of the models used, and for pure alcohol. This positive value is largely caused by dispersion (the dominant part of "others" in the figure) and to a very small degree to MSA. Association and to a lesser extend Born are both negative, but don't fully cancel the strong dispersion term. It is again observed that the RSP-3 contributions show an unphysical extremum in the curves of the electrostatic contributions. The impact of the alcohol content in the solvent is most visible with RSP-2 through the Born term that becomes much more negative for pure alcohol solvent. This is also the expectation, because this activity coefficient is obtained from the derivative with respect to alcohol mole number, and that the Born term is sensitive to this derivative.

To sum up, the corrections for the alcohol and/or salt composition dependence of the RSP model significantly change the behavior of the contributions of the terms in the ePPC-SAFT model to the ionic and solvent activity coefficients; clear unphysical behavior occurs when only the salt composition is corrected for, i.e., in RSP-3. Therefore, although RSP-2, −3, and −4 all present significant improvement on model accuracy for the MIAC of mixed-solvent electrolyte solutions, the analysis on the contributions of terms confirms the preference of RSP-2 over RSP-3 and −4, indicating that correction of the alcohol composition dependence of the RSP is a possible way to improve mixed-solvent electrolyte modeling.

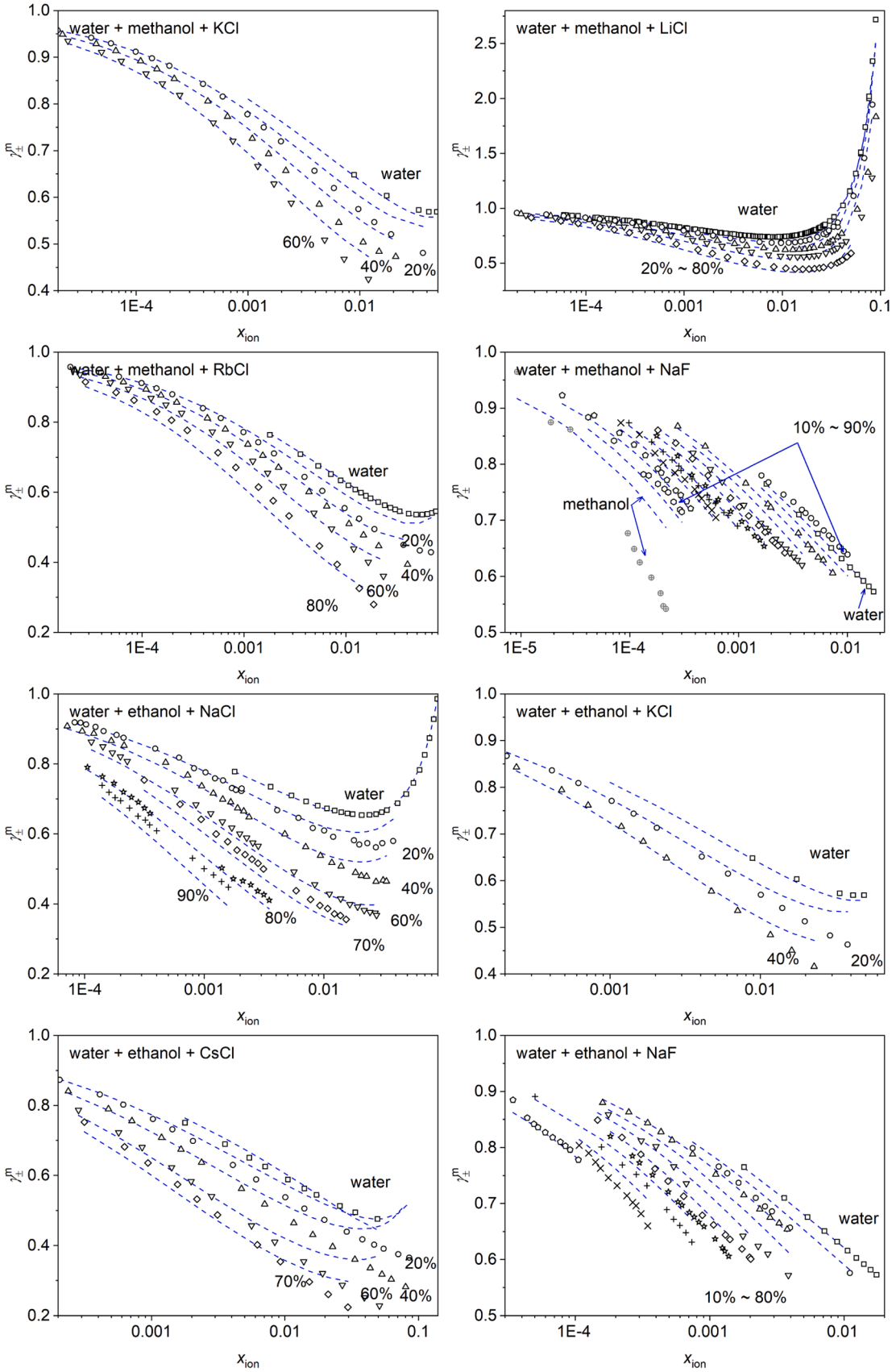

Fig. 6. Comparisons of the MIAC of (water + methanol + KCl), (water + methanol + LiCl), (water + methanol + RbCl), (water + methanol + NaF), (water + ethanol + NaCl), (water + ethanol + KCl), (water + ethanol + CsCl), and (water + ethanol + NaF) calculated using the ePPC-SAFT with RSP-2 (blue dashed lines) at 298.15 K and 0.1 MPa and experimental data (symbols represent salt-free weight fraction of the alcohol, percentages noted in the sub-graphs). Literature of the experimental data is as listed and explained in Section 2.2 and Ref [49].

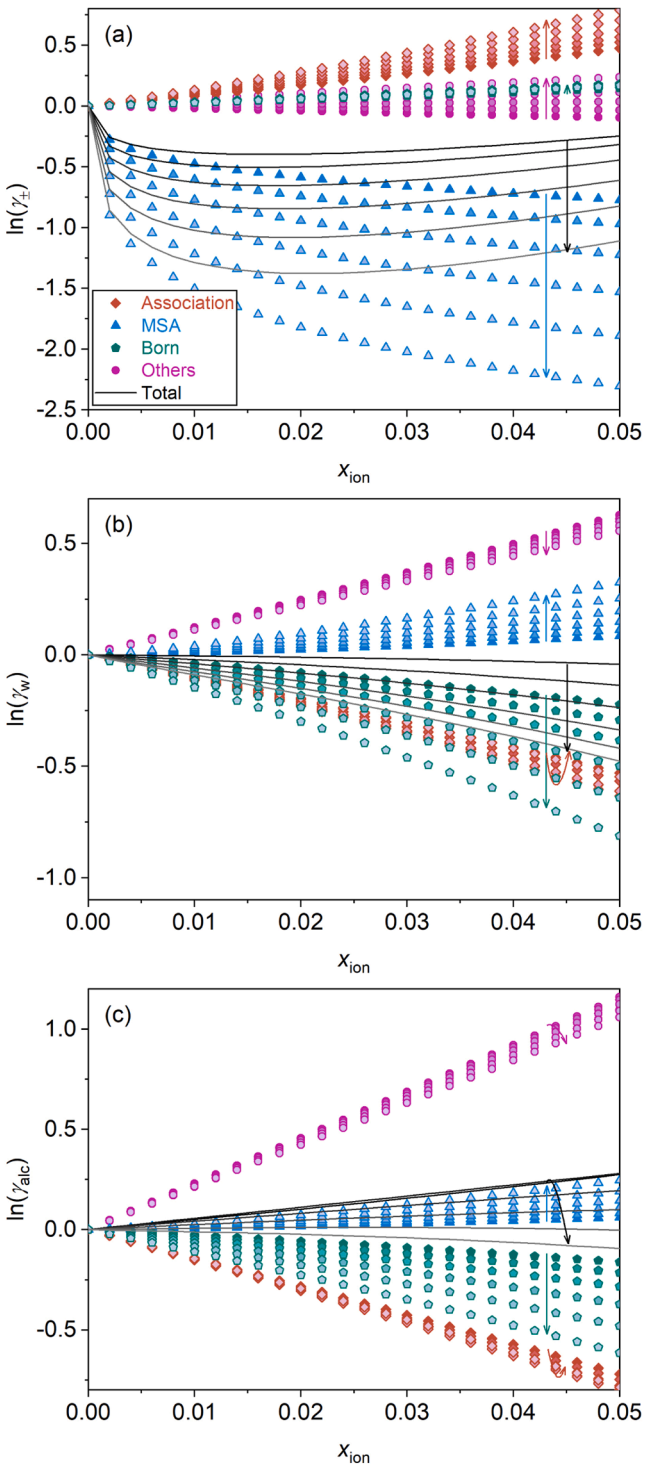

Fig. 7. Contributions to (a) $\ln\gamma_{\pm}$, (b) $\ln\gamma_w$, and (c) $\ln\gamma_{alc}$ of the terms (association, MSA, Born, and others) of ePPC-SAFT combined with RSP-2 for (water + methanol + NaCl) at 298.15 K and 0.1 MPa. The symbols and lines are in gradient colors for salt-free alcohol mole fraction (0%, 20%, 40%, 60%, 80%, 100%), with the higher alcohol compositions in lighter interior colors.

4.3. Mixed-solvent electrolyte solution RSP

In this work, several composition dependence functionalities of the RSP have been investigated. Here we visualize the actual values for this input property. We will not compare the results with the experimental RSP values for the following reasons: 1) Experimental RSP data are very scarce for mixed-solvent electrolyte solutions if not non-existent. 2) A much weaker salt composition dependence of RSP compared to experimental data has been used in our previous works on the aqueous electrolyte solutions [27,28], which agrees with studies focusing on the RSP aspect of aqueous electrolyte EoS modeling [48]. However, we would like to note that the experimental RSP of (water + ethanol + KCl) decreases with both increasing alcohol and salt compositions [120]. Therefore, the discussion will focus on the trends of RSP and how the corrections in alcohol and salt composition dependence take effect. Fig. 8 shows the comparisons of the 4 RSP models for (water + methanol + NaCl) at 298.15 K and 0.1 MPa. RSP-1 and −2 decrease with increasing salt and alcohol compositions. Compared to RSP-1, RSP-2 decreases with alcohol composition more strongly. RSP-2 is smaller for pure methanol compared to RSP-1, which accurately represents the experimental RSP of the solvents. However, we emphasize here that RSP is input rather than output of the primitive electrolyte SAFT model, and that accurate representation of the experimental RSP is not within the scope of the model. RSP-3 increases with salt composition at all alcohol compositions. This is opposite to the experimental trend in aqueous electrolyte solutions, and is likely unphysical for NaCl in the mixed-solvent and in pure alcohol. Similarly, RSP-4 presents a slight increase with salt composition (reversed to the normal trend) at high alcohol composition. However, the unphysical behavior is not as strong as in RSP-3.

4.4. Extrapolation to non-aqueous electrolyte solutions

The model is extrapolated to the non-aqueous electrolyte solutions. The database by Novak et al. [35] is used as a start. Only experimental MIAC are used here. A few datasets are excluded in the comparisons: data from Ref [16] present large scattering; MIAC data are not reported in Ref [121–123]; the mixed-solvent electrolyte MIAC data from the same sources [124–126] were not used after our previous data evaluation [49]. Thus, the following MIAC datasets from the Novak et al. [35] database remain: Ref [127] for (methanol + LiCl) and (methanol + LiBr), Ref [93] for (methanol + NaF), Ref [128] for (methanol + NaI), Ref [129] for (ethanol + LiCl), Ref [129,130] for (ethanol + LiBr), and Ref [131] for (ethanol + NaI). In addition, the osmotic coefficient (OC, ϕ) rather than MIAC were reported in a few references: Ref [132,133] for (methanol + LiCl) and (methanol + LiBr), and Ref [134] for (methanol + KBr). Compared to aqueous and mixed-solvent electrolyte solutions, the data situation for non-aqueous electrolyte solutions is much scarcer. Thus, systematic data evaluations are not possible for these mixtures. On the other hand, our aqueous and mixed-solvent electrolyte model was developed based on critically evaluated databases. In principle, extrapolation to non-aqueous electrolyte solutions should be correct, especially for the cases that MIAC data were used in the parameterization. Furthermore, RSP-2 and −4 present verification on the modeling side. Reliable data are not available for a few of the mixed-solvent electrolyte solution counterparts of these non-aqueous electrolyte solutions. Therefore, the following investigation is limited to the non-aqueous electrolyte solutions for which data are available for the corresponding mixed-solvent electrolyte solutions.

In addition, a few datasets [118,135–140] are included from DETHERM [141]. The OC data from Ref [137] present a strange behavior with a sharp turn-point and near-linear trends on both sides. Therefore, the dataset is excluded in the comparison. Combined with the remaining datasets from the database by Novak et al. [35], the non-aqueous datasets used for comparison here are summarized in the Supplementary Material (Table S5). In a few cases, MIAC was reported along with OC in the isopiestic measurements. The properties are in principle related through the Gibbs-Duhem equation. Then, only OC comparisons are presented in this section for these datasets. The salt composition was reported in molarity in Ref [138], and is converted to mole fraction using density correlations based on experimental density data [142–144]. Fig. 9 shows the MIAC calculated using the ePPC-SAFT model with RSP-2 and −4 and experimental data for (alcohol + salt). For

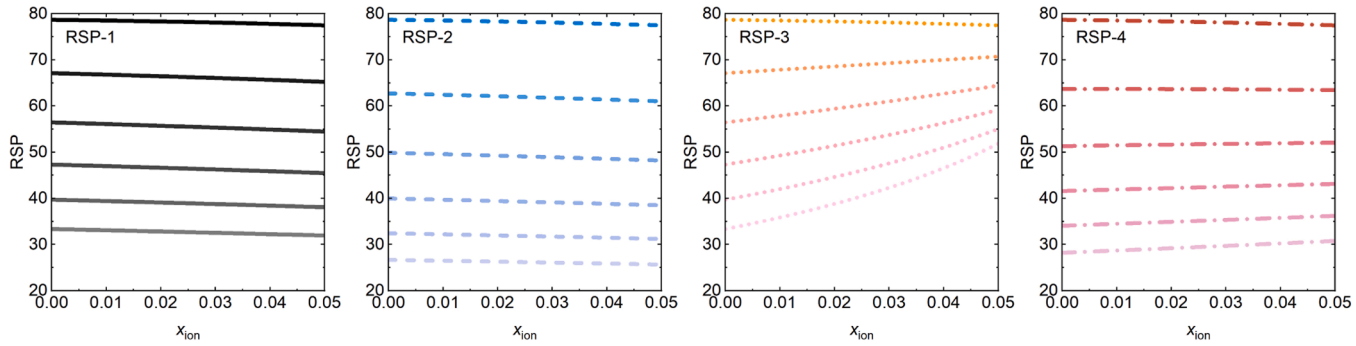

Fig. 8. Comparisons of the 4 RSP models for (water + methanol + NaCl) at 298.15 K and 0.1 MPa. The lines are in gradient colors for salt-free alcohol mole fraction (0%, 20%, 40%, 60%, 80%, 100%), with the higher alcohol compositions in lighter colors.

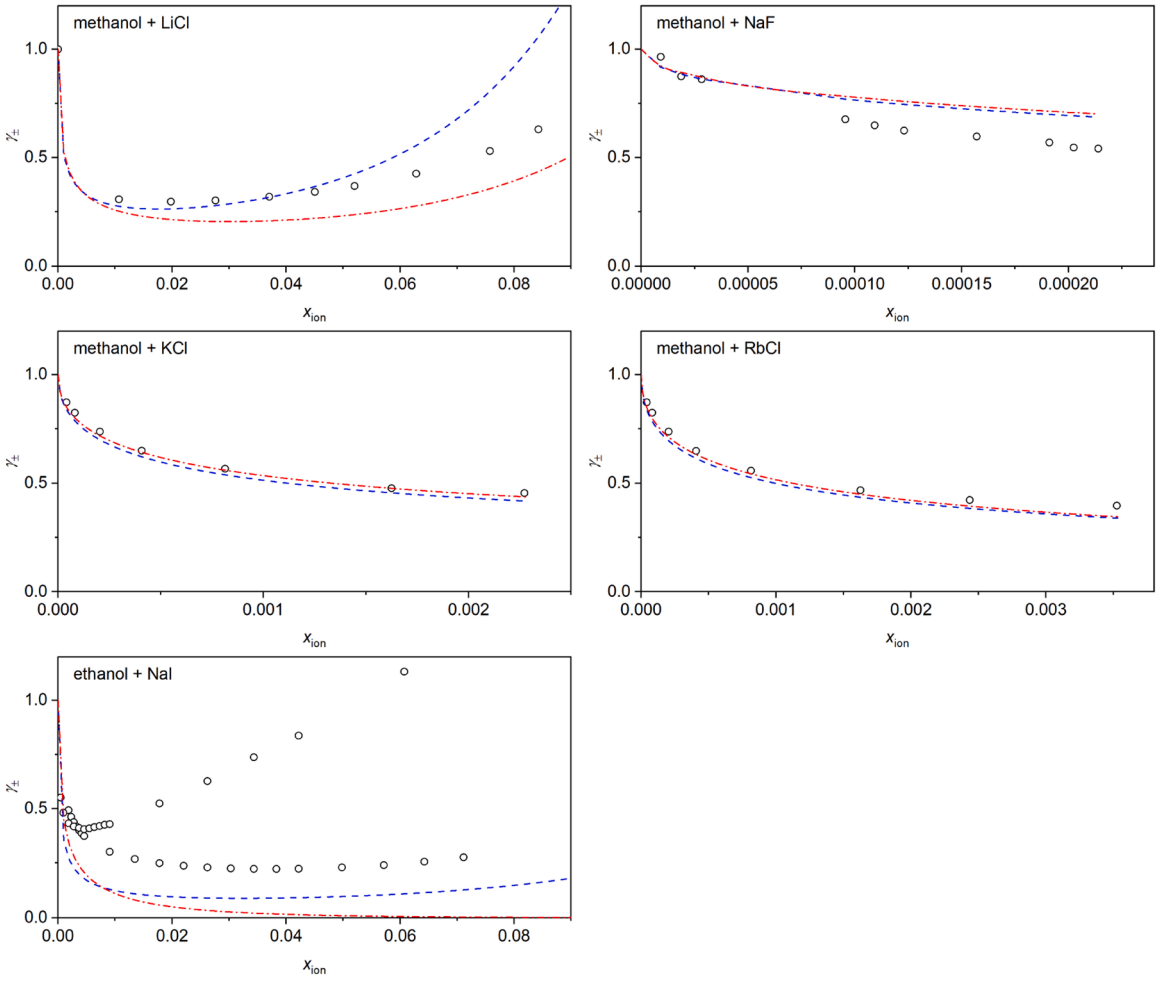

Fig. 9. Comparisons of the MIAC calculated using the ePPC-SAFT model with RSP-2 (blue dashed lines) and RSP-4 (red dash-dotted lines) and experimental data (symbols) for (methanol + LiCl), (methanol + NaF), (methanol + KCl), (methanol + RbCl), and (ethanol + NaI) at 298.15 K and 0.1 MPa.

(methanol + LiCl), RSP-2 accurately predicts the MIAC up to the salt composition at which mixed-solvent electrolyte MIAC data are available at high alcohol composition (80% salt-free alcohol weight fraction), and deviates as salt composition further increases; while RSP-4 underestimates the MIAC. For (water + LiCl), Li^+-water dispersion was included in addition to the association term used for all the other alkali and halide ions in our aqueous electrolyte parameterization [28]. Here, the increase of (methanol + LiCl) MIAC, although not as drastic as in (water + LiCl), further supports the insufficiency of the association term for the short-range Li^+-solvent interaction. The (methanol + NaF) MIAC data are inconsistent with the (water + methanol + NaF) MIAC data (as shown in Fig. 6), much beyond the inconsistency between the aqueous and mixed-solvent solutions of NaF, as discussed in Section 3. For (methanol + KCl) and (methanol + RbCl), both models agree with experimental data very well. This is expected given that the solubility of these salts in methanol is very small. For (ethanol + NaI), the 2 MIAC datasets disagree with each other, both RSP-2 and −4 predict smaller values compared to the experimental data. Considering that only VLE and density data are used in the parameterization of the (water + ethanol + NaI), predictions of the (ethanol + NaI) MIAC are more

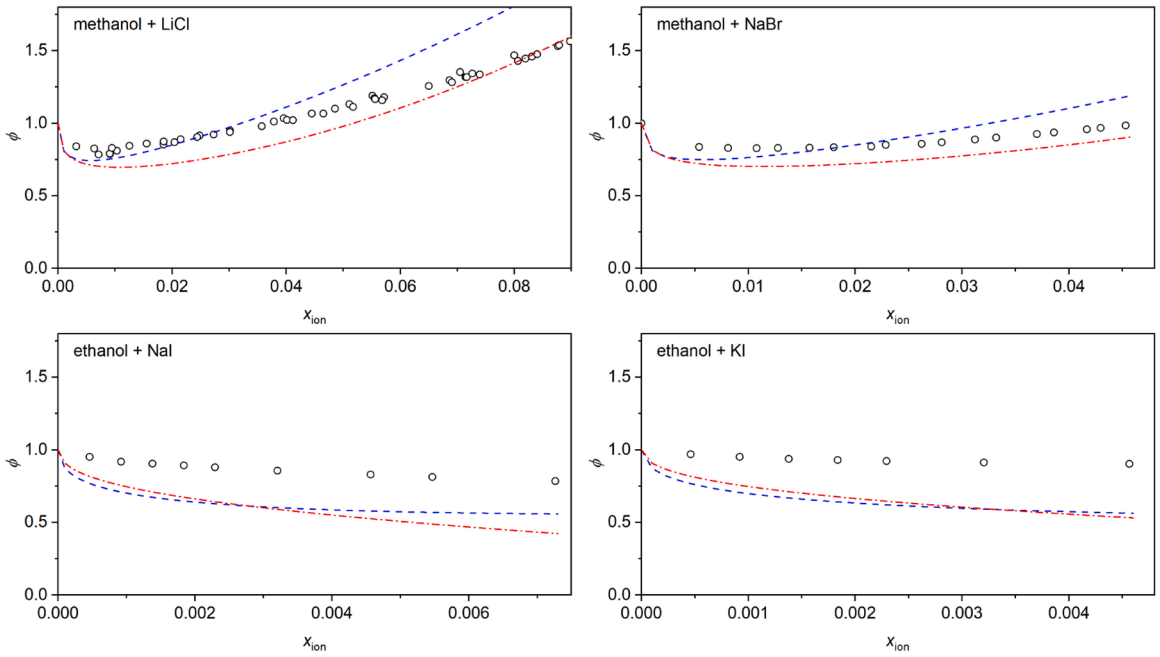

Fig. 10. Comparisons of the OC calculated using the ePPC-SAFT model with RSP-2 (blue dashed lines) and RSP-4 (red dash-dotted lines) and experimental data (symbols) for (methanol + LiCl) and (methanol + NaBr) at 298.15 K and (ethanol + NaI) and (ethanol + KI) at 318.15 K.

challenging compared to the cases for which mixed-solvent electrolyte MIAC data are used in the parameterization. However, the drastic increase of one of the datasets with salt composition is not observed in any of the other non-aqueous electrolyte MIAC or mixed-solvent electrolyte MIAC at high alcohol composition. Overall, considering the data quality of non-aqueous electrolyte MIAC, the extrapolation of the current model is very good.

Fig. 10 shows the OC calculated using the ePPC-SAFT model with RSP-2 and −4 and experimental data for (alcohol + salt). OC is defined only in pure solvents. It was not used in the parameterization of the aqueous electrolyte part of our model, but was used as a test. In principle, OC is related to the solvent activity coefficient, which is further related to the MIAC through the Gibbs-Duhem equation. Here, the few datasets are compared with extrapolations using the ePPC-SAFT with RSP-2 and −4. For (methanol + LiCl) and (methanol + NaBr), the models agree with the experimental data very well. For (methanol + NaBr), considering no mixed-solvent electrolyte MIAC data have been used in the parameterization, the agreement confirms our modeling approach. For (ethanol + NaI) and (ethanol + KI), the models predict smaller values compared to the experimental data. However, there is no distinction of trends at such small salt compositions for further confirmation.

To sum up, the extrapolations of ePPC-SAFT with RSP-2 and −4 show good agreement with experimental data for non-aqueous electrolyte MIAC and OC.

5. Conclusions

The composition dependence of the relative static permittivity (RSP) has been investigated within the framework of ePPC-SAFT. We have shown that extending the ePPC-SAFT with the Schreckenberg RSP model (RSP-1) from aqueous electrolyte solutions to mixed-solvent electrolyte solutions results in accurate representation of the VLE and density, but systematic deviations for MIAC. Efforts are made to improve the MIAC results, by changing the alcohol composition dependence of the RSP (RSP-2), the salt composition dependence in the alcohol (RSP-3), or both (RSP-4). The models are parametrized based on MIAC, VLE, and density. All the parameters are ion-specific. All water-salt and water-alcohol parameters are kept the same as obtained from the binary mixtures. Significant improvements in modeling MIAC are achieved in all 3 approaches, while VLE and density are represented with approximately the same accuracy as the original model. The MIAC results for (water + methanol + NaCl) clearly shows that the alcohol composition dependence of the model must be corrected, suggesting the preference of RSP-2 and −4 over RSP-3, while extrapolations of VLE beyond the salt solubility limits in pure ethanol suggests preference of RSP-2 over RSP-4.

The contribution of the terms to the ionic and solvent activity coefficients are analyzed. Unphysical increase of the MSA contribution to the MIAC is observed for RSP-3, i.e., the case where only the salt composition dependence is corrected. This points to the need to correct the alcohol composition dependence of the RSP model, and confirms the preference for RSP-2. Finally, the RSP using the model parameters obtained from the thermodynamic properties are discussed. Considering the overall performance of the RSP models, we recommend changing the alcohol composition dependence of the RSP (RSP-2) for the mixed-solvent electrolyte solutions.

Potentially, the approach could be used for extending other electrolyte SAFT models to mixed-solvent electrolyte solutions. In this way, a complete re-parametrization of the aqueous electrolyte solutions can be avoided [57].

CRediT authorship contribution statement

Fufang Yang: Writing – original draft, Visualization, Validation, Software, Methodology, Investigation, Formal analysis, Data curation, Conceptualization. **Georgios M. Kontogeorgis:** Writing – review & editing, Supervision, Project administration, Funding acquisition. **Jean-Charles de Hemptinne:** Writing – review & editing, Supervision, Software, Resources, Methodology, Conceptualization.

Declaration of competing interest

The authors declare that they have no known competing financial interests or personal relationships that could have appeared to influence the work reported in this paper.

Data availability

Data will be made available on request.

Acknowledgement

The authors wish to thank the European Research Council (ERC) for funding of this research under European Union's Horizon 2020 research and innovation program (grant agreement No. 832460), ERC Advanced Grant project "New Paradigm in Electrolyte Thermodynamics". FY's attendance at PPEPPD was partially supported by the Otto Mønsteds Fonds.

Supplementary materials

Supplementary material associated with this article can be found, in the online version, at doi:10.1016/j.fluid.2024.114103.

References

[1] M. Bui, C.S. Adjiman, A. Bardow, E.J. Anthony, A. Boston, S. Brown, P.S. Fennell, S. Fuss, A. Galindo, L.A. Hackett, J.P. Hallett, H.J. Herzog, G. Jackson, J. Kemper, S. Krevor, G.C. Maitland, M. Matuszewski, I.S. Metcalfe, C. Petit, G. Puxty, J. Reimer, D.M. Reiner, E.S. Rubin, S.A. Scott, N. Shah, B. Smit, J.P.M. Trusler, P. Webley, J. Wilcox, N.Mac Dowell, Carbon capture and storage (CCS): The way forward, Energy Environ. Sci 11 (2018) 1062–1176, https://doi.org/10.1039/c7ee02342a.

[2] F. Gholami, M. Tomas, Z. Gholami, M. Vakili, Technologies for the nitrogen oxides reduction from flue gas: A review, Sci. Total Environ. 714 (2020) 136712, https://doi.org/10.1016/j.scitotenv.2020.136712.

[3] N.C. Darre, G.S. Toor, Desalination of water: a review, Curr. Pollut. Rep. 4 (2018) 104–111, https://doi.org/10.1007/s40726-018-0085-9.

[4] I.A. Løge, J.R. Bentzon, C.G. Klingaa, J.H. Walther, B.U. Anabaraonye, P. L. Fosbøl, Scale attachment and detachment: The role of hydrodynamics and surface morphology, Chem. Eng. J. 430 (2021) 132583, https://doi.org/10.1016/j.cej.2021.132583.

[5] L.O. Olasunkanmi, Corrosion: Favoured, yet undesirable - Its kinetics and thermodynamics. Corrosion, IntechOpen, London, 2021, pp. 1–17.

[6] Z. Yu, H. Wang, X. Kong, W. Huang, Y. Tsao, D.G. Mackanic, K. Wang, X. Wang, W. Huang, S. Choudhury, Y. Zheng, C.V. Amanchukwu, S.T. Hung, Y. Ma, E. G. Lomeli, J. Qin, Y. Cui, Z. Bao, Molecular design for electrolyte solvents enabling energy-dense and long-cycling lithium metal batteries, Nat. Energy. 5 (2020) 526–533, https://doi.org/10.1038/s41560-020-0634-5.

[7] G.S. Molla, M.F. Freitag, S.M. Stocks, K.T. Nielsen, G. Sin, Solubility Prediction of Different Forms of Pharmaceuticals in Single and Mixed Solvents Using Symmetric Electrolyte Nonrandom Two-Liquid Segment Activity Coefficient Model, Industrial and Engineering Chemistry Research 58 (2019) 4267–4276, https://doi.org/10.1021/acs.iecr.8b04268.

[8] G. Das, M.C. dos Ramos, C. McCabe, Predicting the thermodynamic properties of experimental mixed-solvent electrolyte systems using the SAFT-VR+DE equation of state, Fluid. Phase Equilib. 460 (2018) 105–118, https://doi.org/10.1016/j.fluid.2017.11.017.

[9] L. Blum, D.Q. Wei, Analytical solution of the mean spherical approximation for an arbitrary mixture of ions in a dipolar solvent, J. Chem. Phys. 87 (1987) 555–565, https://doi.org/10.1063/1.453604.

[10] D. Wei, L. Blum, The mean spherical approximation for an arbitrary mixture of ions in a dipolar solvent: Approximate solution, pair correlation functions, and thermodynamics, J. Chem. Phys. 87 (1987) 2999–3007, https://doi.org/10.1063/1.453036.

[11] W. Fürst, H. Renon, Representation of excess properties of electrolyte solutions using a new equation of state, AIChe J. 39 (1993) 335–343, https://doi.org/10.1002/aic.690390213.

[12] J.L. Lebowitz, J.K. Percus, Mean spherical model for lattice gases with extended hard cores and continuum fluids, Phys. Rev. 144 (1966) 251–258, https://doi.org/10.1103/PhysRev.144.251.

[13] P. Debye, E. Hückel, De la theorie des electrolytes. I. abaissement du point de congelation et phenomenes associes, Phys. Z. 24 (1923) 185–206 (in French).

[14] B. Maribo-Mogensen, G.M. Kontogeorgis, K. Thomsen, Comparison of the Debye-Hückel and the mean spherical approximation theories for electrolyte solutions, Ind. Eng. Chem. Res. 51 (2012) 5353–5363, https://doi.org/10.1021/ie2029943.

[15] M. Born, Volumen und hydratationswärme der ionen, Z. Phys. 1 (1920) 45–48 (in German).

[16] C. Held, A. Prinz, V. Wallmeyer, G. Sadowski, Measuring and modeling alcohol/salt systems, Chem. Eng. Sci. 68 (2012) 328–339, https://doi.org/10.1016/j.ces.2011.09.040.

[17] C. Held, T. Reschke, S. Mohammad, A. Luza, G. Sadowski, EPC-SAFT revised, Chem. Eng. Res. Des. 92 (2014) 2884–2897, https://doi.org/10.1016/j.cherd.2014.05.017.

[18] M. Ascani, C. Held, Prediction of salting-out in liquid-liquid two-phase systems with ePC-SAFT: Effect of the Born term and of a concentration-dependent dielectric constant, Z. Anorg. Allg. Chem. 647 (2021) 1305–1314, https://doi.org/10.1002/zaac.202100032.

[19] M. Ascani, G. Sadowski, C. Held, Calculation of Multiphase Equilibria Containing Mixed Solvents and Mixed Electrolytes: General Formulation and Case Studies, J. Chem. Eng. Data. 67 (2022) 1972–1984, https://doi.org/10.1021/acs.jced.1c00866.

[20] T. Van Lingen, V. Bragoni, M. Dyga, B. Exner, D. Schick, C. Held, G. Sadowski, L. J. Gooßen, Carboxylation of Acetylene without Salt Waste: Green Synthesis of C_4 Chemicals Enabled by a CO_2 -Pressure Induced Acidity Switch, Angew Chem Int Ed 62 (2023) e202303882, https://doi.org/10.1002/anie.202303882.

[21] D. Pabsch, J. Lindfeld, J. Schwalm, A. Strangmann, P. Figiel, G. Sadowski, C. Held, Influence of solvent and salt on kinetics and equilibrium of esterification reactions, Chem. Eng. Sci. 263 (2022) 118046, https://doi.org/10.1016/j.ces.2022.118046.

[22] D. Schick, Q. Chen, L. Hellfajer, A. Strangmann, P. Figiel, J.P.M. Trusler, G. Sadowski, C. Held, Influence of Solvents and Salts on CO_2 Solubility and the Impact on an Esterification Reaction, J. Chem. Eng. Data. (2023), https://doi.org/10.1021/acs.jced.3c00178 acs.jced.3c00178.

[23] M. Ascani, D. Pabsch, M. Klinksiek, N. Gajardo-Parra, G. Sadowski, C. Held, Prediction of pH in multiphase multicomponent systems with ePC-SAFT advanced, Chem. Commun. 58 (2022) 8436–8439, https://doi.org/10.1039/D2CC02943J.

[24] J.M.A. Schreckenberg, S. Dufal, A.J. Haslam, C.S. Adjiman, G. Jackson, A. Galindo, Modelling of the thermodynamic and solvation properties of electrolyte solutions with the statistical associating fluid theory for potentials of variable range, Mol. Phys. 112 (2014) 2339–2364, https://doi.org/10.1080/00268976.2014.910316.

[25] S. Ahmed, N. Ferrando, J.C. de Hemptinne, J.P. Simonin, O. Bernard, O. Baudouin, Modeling of mixed-solvent electrolyte systems, Fluid. Phase Equilib. 459 (2018) 138–157, https://doi.org/10.1016/j.fluid.2017.12.002.

[26] J.S. Roa Pinto, N. Ferrando, J.C. de Hemptinne, A. Galindo, Temperature dependence and short-range electrolytic interactions within the e-PPC-SAFT framework, Fluid. Phase Equilib. 560 (2022) 113486, https://doi.org/10.1016/j.fluid.2022.113486.

[27] F. Yang, T.D. Ngo, J.S. Roa Pinto, G.M. Kontogeorgis, J.C. De Hemptinne, Systematic evaluation of parameterization approaches for the ePPC-SAFT model for aqueous alkali halide solutions, Fluid. Phase Equilib. 570 (2023) 113778.

[28] F. Yang, G.M. Kontogeorgis, J.C. de Hemptinne, Systematic evaluation of parameterization approaches for the ePPC-SAFT model for aqueous alkali halide solutions. II. 15 salts involving F-, Br-, I-, and Li+ ions, Fluid. Phase Equilib. 573 (2023) 113853.

[29] B. Maribo-Mogensen, K. Thomsen, G.M. Kontogeorgis, An electrolyte CPA equation of state for mixed solvent electrolytes, AIChe J. 61 (2015) 2933–2950, https://doi.org/10.1002/aic.14829.

[30] D.K. Eriksen, G. Lazarou, A. Galindo, G. Jackson, C.S. Adjiman, A.J. Haslam, Development of intermolecular potential models for electrolyte solutions using an electrolyte SAFT-VR Mie equation of state, Mol. Phys. 114 (2016) 2724–2749, https://doi.org/10.1080/00268976.2016.1236221.

[31] M.D. Olsen, G.M. Kontogeorgis, X. Liang, N. von Solms, Comparison of models for the relative static permittivity with the e-CPA equation of state, Fluid. Phase Equilib. 565 (2023) 113632, https://doi.org/10.1016/j.fluid.2022.113632.

[32] M.D. Olsen, G.M. Kontogeorgis, J.C. De Hemptinne, X. Liang, N. Von Solms, Comparisons of equation of state models for electrolytes: e-CPA and e-PPC-SAFT, Fluid. Phase Equilib. 571 (2023) 113804, https://doi.org/10.1016/j.fluid.2023.113804.

[33] H. Zhao, M.C. Dos Ramos, C. McCabe, Development of an equation of state for electrolyte solutions by combining the statistical associating fluid theory and the mean spherical approximation for the nonprimitive model, J. Chem. Phys. 126 (2007) 244503, https://doi.org/10.1063/1.2733673.

[34] N. Novak, G.M. Kontogeorgis, M. Castier, I.G. Economou, Mixed solvent electrolyte solutions: a review and calculations with eSAFT-VR Mie Equations of State, Submitted for Publication. (2023).

[35] N. Novak, G.M. Kontogeorgis, M. Castier, I.G. Economou, Extension of the eSAFT-VR Mie equation of state from aqueous to non-aqueous electrolyte solutions, Fluid. Phase Equilib. 565 (2023) 113618, https://doi.org/10.1016/j.fluid.2022.113618.

[36] J.R. Loehe, M.D. Donohue, Recent advances in modeling thermodynamic properties of aqueous strong electrolyte systems, AIChe J. 43 (1997) 180–195, https://doi.org/10.1002/aic.690430121.

[37] G.M. Kontogeorgis, B. Maribo-Mogensen, K. Thomsen, The Debye-Hückel theory and its importance in modeling electrolyte solutions, Fluid. Phase Equilib. 462 (2018) 130–152, https://doi.org/10.1016/j.fluid.2018.01.004.

[38] C. Held, Thermodynamic g E models and equations of state for electrolytes in a water-poor medium: A review, J. Chem. Eng. Data. 65 (2020) 5073–5082, https://doi.org/10.1021/acs.jced.0c00812.

[39] Y. Marcus, Electrostriction in Electrolyte Solutions, Chem. Rev. 111 (2011) 2761–2783, https://doi.org/10.1021/cr100130d.

[40] J. Mähler, I. Persson, A study of the hydration of the alkali metal ions in aqueous solution, Inorg. Chem. 51 (2012) 425–438, https://doi.org/10.1021/ic2018693.

[41] R. t Shannon, C. Prewitt, Revised values of effective ionic radii, Acta Crystallogr. B Struct. Crystallogr. Cryst. Chem. 26 (1970) 1046–1048.

[42] R.D. Shannon, Revised effective ionic radii and systematic studies of interatomic distances in halides and chalcogenides, Acta Crystallographica Section A: Crystal Physics, Diffraction, Theoretical and General Crystallography 32 (1976) 751–767.

[43] L. Pauling, The Nature of the Chemical Bond and the Structure of Molecules and crystals: an Introduction to Modern Structural Chemistry, Cornell University Press, Ithaca, NY, 1939.
[44] J. Rozmus, J.C. De Hemptinne, A. Galindo, S. Dufal, P. Mougin, Modeling of strong electrolytes with ePPC-SAFT up to high temperatures, Ind. Eng. Chem. Res. 52 (2013) 9979–9994, https://doi.org/10.1021/ie303527j.
[45] S. Ahmed, N. Ferrando, J.C. De Hemptinne, J.P. Simonin, O. Bernard, O. Baudouin, A New PC-SAFT Model for Pure Water, Water-Hydrocarbons, and Water-Oxygenates Systems and Subsequent Modeling of VLE, VLLE, and LLE, J. Chem. Eng. Data. 61 (2016) 4178–4190, https://doi.org/10.1021/acs.jced.6b00565.
[46] K. Giese, U. Kaatze, R. Pottel, Permittivity and dielectric and proton magnetic relaxation of aqueous solutions of the alkali halides, J. Phys. Chem. 74 (1970) 3718–3725.
[47] J.P. Simonin, O. Bernard, L. Blum, Real ionic solutions in the mean spherical approximation. 3. Osmotic and activity coefficients for associating electrolytes in the primitive model, J. Phys. Chem. B. 102 (1998) 4411–4417, https://doi.org/10.1021/jp9732423.
[48] B. Maribo-Mogensen, G.M. Kontogeorgis, K. Thomsen, Modeling of dielectric properties of aqueous salt solutions with an equation of state, J. Phys. Chem. B. 117 (2013) 10523–10533, https://doi.org/10.1021/jp403375t.
[49] F. Yang, T.D. Ngo, G.M. Kontogeorgis, J.C. De Hemptinne, A benchmark database for mixed-solvent electrolyte solutions: Consistency analysis using E-NRTL, Ind. Eng. Chem. Res. 61 (2022) 15576–15593.
[50] F. Yang, J. Qu, G.M. Kontogeorgis, J.C. De Hemptinne, Reference density database for 20 aqueous alkali halide solutions, J. Phys. Chem. Ref. Data. 51 (2022) 043104.
[51] P.K. Jog, S.G. Sauer, J. Blaesing, W.G. Chapman, Application of dipolar chain theory to the phase behavior of polar fluids and mixtures, Ind. Eng. Chem. Res. 40 (2001) 4641–4648, https://doi.org/10.1021/ie010264. +.
[52] D. NguyenHuynh, J.P. Passarello, P. Tobaly, J.C. de Hemptinne, Application of GC-SAFT EOS to polar systems using a segment approach, Fluid. Phase Equilib. 264 (2008) 62–75, https://doi.org/10.1016/j.fluid.2007.10.019.
[53] K.E. Gubbins, C.H. Twu, Thermodynamics of polyatomic fluid mixtures-I theory, Chem. Eng. Sci. 33 (1978) 863–878, https://doi.org/10.1016/0009-2509(78)85176-8.
[54] T.K.H. Trinh, J.P. Passarello, J.C. de Hemptinne, R. Lugo, Use of a non additive GC-PPC-SAFT equation of state to model hydrogen solubility in oxygenated organic compounds, Fluid. Phase Equilib. 429 (2016) 177–195, https://doi.org/10.1016/j.fluid.2016.08.003.
[55] M. Holz, H. Weingärtner, H.G. Hertz, Nuclear magnetic relaxation of alkali halide nuclei and preferential solvation in methanol + water mixtures, J. Chem. Soc., Faraday Trans. 1. 73 (1977) 71, https://doi.org/10.1039/f19777300071.
[56] J.R. Graham, G.S. Kell, A.R. Gordon, Equivalent and Ionic Conductances for Lithium, Sodium and Potassium Chlorides in Anhydrous Ethanol at 25 °, J. Am. Chem. Soc. 79 (1957) 2352–2355, https://doi.org/10.1021/ja01567a003.
[57] P.S. Albright, L.J. Gosting, Dielectric constants of the methanol-water system from 5 to 55o, J. Am. Chem. Soc. 68 (1946) 1061–1063.
[58] D. Nguyen-Huynh, J.C. De Hemptinne, R. Lugo, J.P. Passarello, P. Tobaly, Modeling Liquid–Liquid and Liquid–Vapor Equilibria of Binary Systems Containing Water with an Alkane, an Aromatic Hydrocarbon, an Alcohol or a Gas (Methane, Ethane, CO_2 or H_2S), Using Group Contribution Polar Perturbed-Chain Statistical Associating Fluid Theory, Ind. Eng. Chem. Res. 50 (2011) 7467–7483, https://doi.org/10.1021/ie102045g.
[59] J.A. Schroeder, S.G. Penoncello, J.S. Schroeder, A Fundamental Equation of State for Ethanol, J. Phys. Chem. Ref. Data 43 (2014) 043102, https://doi.org/10.1063/1.4895394.
[60] H.J.E. Dobson, The Partial Pressures of Aqueous Ethyl Alcohol, Journal of Chemical Society 127 (1925) 2866–2873.
[61] R.C. Pemberton, C.J. Mash, Thermodynamic properties of aqueous non-electrolyte mixtures II. Vapour pressures and excess Gibbs energies for water + ethanol at 303.15 to 363.15 K determined by an accurate static method, The Journal of Chemical Thermodynamics 10 (1978) 867–888, https://doi.org/10.1016/0021-9614(78)90160-X.
[62] L. Zhang, Y. Ge, D. Ji, J. Ji, Experimental measurement and modeling of vapor-liquid equilibrium for ternary systems containing ionic liquids: A case study for the system water + ethanol + 1-hexyl-3-methylimidazolium chloride, J. Chem. Eng. Data 54 (2009) 2322–2329, https://doi.org/10.1021/je900002p.
[63] P.A. Nelson, A.E. Markham, Vapor-liquid equilibrium of pyridine-acetic anhydride solutions, J. Am. Chem. Soc. 72 (1950) 2417–2418.
[64] R. Sun, Calculation of salting effect on vapor-liquid equilibrium in water-nonelectrolyte systems, Chemical Engineering (China) 23 (1995) 13–17, 30 (in Chinese).
[65] K. Iwakabe, H. Kosuge, Isobaric vapor-liquid-liquid equilibria with a newly developed still, Fluid. Phase Equilib. 192 (2001) 171–186, https://doi.org/10.1016/S0378-3812(01)00631-8.
[66] Q. Li, W. Zhu, H. Wang, X. Ran, Y. Fu, B. Wang, Isobaric vapor-liquid equilibrium for the ethanol + water + 1,3-dimethylimidazolium dimethylphosphate system at 101.3 kPa, J. Chem. Eng. Data 57 (2012) 696–700, https://doi.org/10.1021/je2005209.
[67] E.C. Voutsas, C. Pamouktsis, D. Argyris, G.D. Pappa, Measurements and thermodynamic modeling of the ethanol-water system with emphasis to the azeotropic region, Fluid. Phase Equilib. 308 (2011) 135–141, https://doi.org/10.1016/j.fluid.2011.06.009.
[68] H.S. Lai, Y.F. Lin, C.H. Tu, Isobaric (vapor + liquid) equilibria for the ternary system of (ethanol + water + 1,3-propanediol) and three constituent binary systems at P = 101.3 kPa, Journal of Chemical Thermodynamics 68 (2014) 13–19, https://doi.org/10.1016/j.jct.2013.08.020.
[69] C. Tsanas, A. Tzani, A. Papadopoulos, A. Detsi, E. Voutsas, Ionic liquids as entrainers for the separation of the ethanol/water system, Fluid. Phase Equilib. 379 (2014) 148–156, https://doi.org/10.1016/j.fluid.2014.07.022.
[70] N. Kamihama, H. Matsuda, K. Kurihara, K. Tochigi, S. Oba, Isobaric vapor-liquid equilibria for ethanol + water + ethylene glycol and its constituent three binary systems, J. Chem. Eng. Data 57 (2012) 339–344, https://doi.org/10.1021/je2008704.
[71] R.M. Rieder, A.R. Thompson, Vapor-Liquid Equilibria Measured by a Gillespie Still - Ethyl Alcohol - Water System, Industrial & Engineering Chemistry 41 (1949) 2905–2908, https://doi.org/10.1021/ie50480a060.
[72] A. Arce, J. Martínez-Ageitos, A. Soto, VLE for water + ethanol + 1-octanol mixtures. Experimental measurements and correlations, Fluid. Phase Equilib. 122 (1996) 117–129, https://doi.org/10.1016/0378-3812(96)03041-5.
[73] A. Auger, N. Hansen, A Restart CMA Evolution Strategy With Increasing Population Size, in: 2005 IEEE Congress on Evolutionary Computation, IEEE, Edinburgh, Scotland, UK, 2005, pp. 1769–1776, https://doi.org/10.1109/CEC.2005.1554902.
[74] D. Nguyen-Huynh, J.P. Passarello, P. Tobaly, J.C. De Hemptinne, Modeling Phase Equilibria of Asymmetric Mixtures Using a Group-Contribution SAFT (GC-SAFT) with a k_{ij} Correlation Method Based on London's Theory. 1. Application to CO_2 + n -Alkane, Methane + n -Alkane, and Ethane + n -Alkane Systems, Ind. Eng. Chem. Res. 47 (2008) 8847–8858, https://doi.org/10.1021/ie071643r.
[75] J.A.V. Butler, D.W. Thomsen, W.H. Maclennan, The free energy of the normal aliphatic in aqueous solution. Part I. The partial vapor pressures of aqueous solutions of methyl, n-propyl, and n-butyl alcohols in water. Part II. The solubilities of some normal aliphatic alcohols in water. Part III. The t, Journal of Chemical Society (1933) 674–686.
[76] Z. Bao, M. Liu, J. Yang, N. Wang, Measurement and correlation of moderate pressure vapor-liquid equilibrium data for methanol-water binary system, CIESC Journal 46 (1995) 230–233.
[77] K. Kurihara, T. Minoura, K. Takeda, K. Kojima, Isothermal Vapor-Liquid Equilibria for Methanol + Ethanol + Water, Methanol + Water, and Ethanol + Water, Journal of Chemical and Engineering Data. 40 (1995) 679–684, https://doi.org/10.1021/je00019a033.
[78] Advanced Tools for Optimization and Uncertainty Treatment, (2019).
[79] H.S. Harned, A rule for the calculation of the activity coefficients of salts in organic solvent-water mixtures, Journal of Physical Chemistry 66 (1962) 589–591, https://doi.org/10.1021/j100810a004.
[80] P.R. Mussini, T. Mussini, B. Sala, Thermodynamics of the cell {Li-Amalgam | LiX (m)| AgX | Ag} (X = Cl,Br) and medium effects upon LiX in (acetonitrile + water), (1,4-dioxane + water), and (methanol + water) solvent mixtures with related solvation parameters, Journal of Chemical Thermodynamics 32 (2000) 597–616, https://doi.org/10.1006/jcht.1999.0622.
[81] A. Basili, P.R. Mussini, T. Mussini, S. Rondinini, B. Sala, A. Vertova, Transference numbers of alkali chlorides and characterization of salt bridges for use in methanol+water mixed solvents, J. Chem. Eng. Data 44 (1999) 1002–1008, https://doi.org/10.1021/je9900979.
[82] M. Hu, J. Tang, S. Li, S. Xia, Y. Jiang, Activity coefficients of lithium chloride in ROH/water mixed solvent (R = Me, Et) using the electromotive force method at 298.15 K, J. Chem. Eng. Data 53 (2008) 508–512, https://doi.org/10.1021/je700614h.
[83] M. Broul, K. Hlavatý, J. Linek, Liquid-vapour equilibrium in systems of electrolytic components. V. The system CH3OH-H2O-LiCl at 60°C, Collect. Czech. Chem. Commun 34 (1969) 3428–3435.
[84] Y. Xu, S. Li, Q. Zhai, Y. Jiang, M. Hu, Investigation on the thermodynamic properties of KCl/CsCl + NaCl + CH3OH + H2O quaternary systems at 298.15 K, Journal of Industrial and Engineering Chemistry 20 (2014) 2159–2165, https://doi.org/10.1016/j.jiec.2013.09.046.
[85] A. Basili, P.R. Mussini, T. Mussini, S. Rondinini, Thermodynamics of the cell: {NaxHg1-x|NaCl(m)|AgCl|Ag} in (methanol + water) solvent mixtures, Journal of Chemical Thermodynamics 28 (1996) 923–933, https://doi.org/10.1006/jcht.1996.0081.
[86] J. Yao, W.D. Yan, Y.J. Xu, S.J. Han, Activity coefficients for NaCl in MeOH + H2O by electromotive force measurements at 308.15 K and 318.15 K, J. Chem. Eng. Data. 44 (1999) 497–500, https://doi.org/10.1021/je970288g.
[87] F. Hernández-Hernández, F. Pérez-Villaseñor, V. Hernández-Ruiz, G.A. Iglesias-Silva, Activity coefficients of NaCl in H2O + MeOH + EtOH by electromotive force at 298.15 K, J. Chem. Eng. Data 52 (2007) 959–964, https://doi.org/10.1021/je600549h.
[88] S.O. Yang, C.S. Lee, Vapor-liquid equilibria of water + methanol in the presence of mixed salts, J. Chem. Eng. Data 43 (1998) 558–561, https://doi.org/10.1021/je970286w.
[89] J. Yao, H. Li, S. Han, Vapor-liquid equilibrium data for methanol-water-NaCl at 45°C, Fluid. Phase Equilib. 162 (1999) 253–260, https://doi.org/10.1016/S0378-3812(99)00204-6.
[90] A.I. Johnson, W.F. Furter, Salt Effect in Vapor-Liquid Equilibrium, Canadian Journal of Chemical Engineering 38 (1960) 78–87.
[91] A. Basili, P.R. Mussini, T. Mussini, S. Rondinini, A. Vertova, Thermodynamics of the amalgam cell: {MexHg1-x|MeCl(m)| AgCl| Ag} (with Me = K, Rb) in (methanol+water) solvent mixtures, Berichte Der Bunsengesellschaft Für Physikalische Chemie 101 (1997) 842–846, https://doi.org/10.1002/bbpc.19971010510.
[92] J. Zhang, S.Y. Gao, S.P. Xia, Y. Yao, Study of thermodynamic properties of quaternary mixture RbCl + Rb2SO4 + CH 3OH + H2O by EMF measurement at

298.15 K, Fluid. Phase Equilib. 226 (2004) 307–312, https://doi.org/10.1016/j.fluid.2004.10.010.
[93] F. Hernández-Luis, M.V. Vázquez, M.A. Esteso, Activity coefficients for NaF in methanol-water and ethanol-water mixtures at 25°C, J. Mol. Liq. 108 (2003) 283–301, https://doi.org/10.1016/S0167-7322(03)00187-9.
[94] M.A. Esteso, O.M. Gonzalez-Diaz, F.F. Hernandez-Luis, L. Fernandez-Merida, Activity coefficients for NaCl in ethanol-water mixtures at 25 C, J. Solution. Chem. 18 (1989) 277–288.
[95] M.N. Mamontov, N.M. Konstantinova, I.A. Uspenskaya, Water-ethanol-sodium chloride system: The main sources of uncertainties in thermodynamic properties determined by potentiometry, Fluid. Phase Equilib. 412 (2016) 62–70, https://doi.org/10.1016/j.fluid.2015.12.012.
[96] R. Yang, J. Demirgian, J.F. Solsky, E.J. Kikta, J.A. Marinsky, Mean molal activity of sodium chloride, potassium chloride, and cesium chloride in ethanol-water mixtures, Journal of Physical Chemistry 83 (1979) 2752–2761, https://doi.org/10.1021/j100484a013.
[97] T. Meyer, H.M. Poika, J. Gmehling, Low-Pressure Isobarle Vapor-Liquid Equilibria of Ethanol/Water Mixtures Containing Electrolytes, J. Chem. Eng. Data 36 (1991) 340–342, https://doi.org/10.1021/je00003a023.
[98] P.R. Mussini, T. Mussini, A. Perelli, S. Rondinini, A. Vertova, Thermodynamics of the cell: {MexHg1−x|MeCl(m)|AgCl|Ag} (Me = Na,K,Cs) in (ethanol + water) solvent mixtures, The Journal of Chemical Thermodynamics 27 (1995) 245–251, https://doi.org/10.1006/jcht.1995.0022.
[99] R. Sun, Molecular thermodynamics of salt effect in vapor-liquid equilibrium - Calculation of isobaric VLE salt effect parameters for ethanol-water-1-1 type electrolyte systems, CIESC Journal 47 (1996) 401–409 (in Chinese).
[100] J.A. Burns, W.F. Furter, Effects of Salts Having Large Organic Ions on Vapor-Liquid Equilibrium, in: Advances in Chemistry, Thermodynamic Behavior of Electrolytes in Mixed Solvents, AMERICAN CHEMICAL SOCIETY (1976) 99–127, https://doi.org/10.1021/ba-1976-0155.ch008.
[101] H. Yamamoto, T. Terano, M. Yanagisawa, J. Tokunaga, Y. Nishi, J. Tokunaga, Salt effect of CACL2, NH4i and NAI on vapor-liquid equilibrium of ethanol + water system at 298.15 K, Can. J. Chem. Eng. 73 (1995) 779–783, https://doi.org/10.1002/cjce.5450730522.
[102] J.A. Burns, W.F. Furter, Salt Effect in Vapor-Liquid Equilibrium At Fixed Liquid Composition, Advances in Chemistry Series (1979) 11–26, https://doi.org/10.1021/ba-1979-0177.ch002.
[103] H.H. Emons, H. Roser, Untersuchungen an Systemen aus Salzen und gemischten Losungsmitteln. III. Die Beeinflussung der Systeme Kaliumsulfat- bzw. Natriumsulfat-Alkohol-Wasser durch Zusatz von Natrium- oder Kaliumchlorid, Z. Anorg. Allg. Chem. 353 (1967) 135–147, https://doi.org/10.1002/zaac.19673530305 (in German).
[104] J.O. Bockris, H. Egan, The salting-out effect and dielectric constant, Trans. Faraday Soc. 44 (1948) 151–159.
[105] T. Guetachew, S. Ye, I. Mokbel, J. Jose, P. Xans, Study of NaCl solutions in a mixed solvent H2O-CH3OH: Experimental densities and comparison with calculated values obtained with a modified Pitzer's model, J. Solution. Chem. 25 (1996) 895–903, https://doi.org/10.1007/BF00972580.
[106] M. Kohns, M. Horsch, H. Hasse, Partial molar volume of NaCl and CsCl in mixtures of water and methanol by experiment and molecular simulation, Fluid. Phase Equilib. 458 (2018) 30–39, https://doi.org/10.1016/j.fluid.2017.10.034.
[107] W. Herz, G. Anders, Uber Loslichkeiten in Losungsmittelgemengen V, Z. Anorg. Chem. 55 (1907) 271–278 (in German).
[108] N. Takenaka, T. Takemura, M. Sakurai, Partial Molal Volumes of Uni-univalent Electrolytes in Methanol + Water. 2. Sodium Bromide and Potassium Bromide, J. Chem. Eng. Data. 39 (1994) 796–801, https://doi.org/10.1021/je00016a036.
[109] L. Werblan, Viscous flow mechanisms in water-methanol solutions of alkali metal halides. I, Bull. Acad. Pol. Sci., Sér. Sci. Chim. 27 (1979) 873–890.
[110] H.E. Armstrong, J.V. Eyre, A.V. Hussey, W.P. Paddison, Studies of the processes operative in solutions. - Parts II-V, Proc. R. Soc. London. 79 (1907) 564–597.
[111] H.R. Galleguillos, M.E. Taboada, T.A. Graber, S. Bolado, Compositions, Densities, and Refractive Indices of Potassium Chloride + Ethanol + Water and Sodium Chloride + Ethanol + Water Solutions at (298.15 and 313.15) K, J. Chem. Eng. Data. 48 (2003) 405–410, https://doi.org/10.1021/je020173z.
[112] J. Cao, Y. Ren, J. Liu, Solid–Liquid Phase Equilibria of the KH $_2$ PO $_4$ –KCl–H $_3$ PO $_4$ –H $_2$ O and KH $_2$ PO $_4$ –KCl–C $_2$ H $_5$ OH–H $_2$ O Systems at T = (298.15 and 313.15) K, J. Chem. Eng. Data. 63 (2018) 2065–2074, https://doi.org/10.1021/acs.jced.8b00081.
[113] W.X. Zhao, M.C. Hu, Y.C. Jiang, S.N. Li, Solubilities, densities and refractive indices of rubidium chloride or cesium chloride in ethanol aqueous solutions at different temperatures, Chin. J. Chem. 25 (2007) 478–483, https://doi.org/10.1002/cjoc.200790090.
[114] B. Nowicka, A. Kacperska, J. Barczyńska, A. Bald, S. Taniewska-Osińska, Viscosity of solutions of NaI and CaCl2 in water-ethanol and of NaI in water-tetrahydrofuran mixtures, J. Chem. Soc., Faraday Trans. 1. 84 (1988) 3877–3884, https://doi.org/10.1039/F19888403877.
[115] R.R. Pawar, S.B. Nahire, M. Hasan, Solubility and density of potassium iodide in binary ethanol-water solvent mixture at (298.15, 303.15, 308.15, and 313.15) K, J. Chem. Eng. Data. 54 (2009) 1935–1937, https://doi.org/10.1021/je800682p.
[116] J. Barthel, R. Neueder, G. Lauermann, Vapor pressures of non-aqueous electrolyte solutions. Part 1. Alkali metal salts in methanol, J. Solution. Chem. 14 (1985) 621–633, https://doi.org/10.1007/BF00646055.
[117] W. Yan, Y. Xu, S. Han, A new method of pseudo-static ebulliometer for determination of osmotic coefficients of nonaqueous electrolyte solution, Acta Physico Chimica Sinica 11 (1995) 454–459 (in Chinese).
[118] F. Mato, M.J. Cocero, Measurement of Vapor Pressures of Electrolyte Solutions by Vapor Pressure Osmometry, J. Chem. Eng. Data 33 (1988) 38–39, https://doi.org/10.1021/je00051a013.
[119] S. Vaque Aura, J.S. Roa Pinto, N. Ferrando, J.C. De Hemptinne, A. ten Kate, S. Kuitunen, N. Diamantonis, T. Gerlach, M. Heilig, G. Becker, M. Brehelin, Data analysis for electrolyte systems: A method illustrated on alkali halides in water, J. Chem. Eng. Data. 66 (2021) 2976–2990, https://doi.org/10.1021/acs.jced.1c00105.
[120] J. Barthel, R. Buchner, Electrolyte Data Collection: Dielectric Properties of Water and Aqueous Electrolyte Solutions, DECHEMA, Frankfurt, 1995.
[121] L. Malahias, O. Popovych, Activity Coefficients and Transfer Free Energies of Potassium Chloride in Methanol-Water Solvents at 25°C, J. Chem. Eng. Data 27 (1982) 105–109, https://doi.org/10.1021/je00028a001.
[122] M.Y. Li, L.S. Wang, K.P. Wang, B. Jiang, J. Gmehling, Experimental measurement and modeling of solubility of LiBr and LiNO3 in methanol, ethanol, 1-propanol, 2-propanol and 1-butanol, Fluid. Phase Equilib. 307 (2011) 104–109, https://doi.org/10.1016/j.fluid.2011.03.017.
[123] B. Long, D. Zhao, W. Liu, Thermodynamics Studies on the Solubility of Inorganic Salt in Organic Solvents: Application to KI in Organic Solvents and Water–Ethanol Mixtures, Ind. Eng. Chem. Res. 51 (2012) 9456–9467, https://doi.org/10.1021/ie301000b.
[124] S. Han, H. Pan, Thermodynamics of the sodium bromide-methanol-water and sodium bromide-ethanol-water two ternary systems by the measurements of electromotive force at 298.15 K, Fluid. Phase Equilib. 83 (1993) 261–270, https://doi.org/10.1016/0378-3812(93)87029-Z.
[125] O.M. González-Díaz, L. Fernández-Mérida, F. Hernández-Luis, M.A. Esteso, Activity coefficients for NaBr in ethanol-water mixtures at 25°C, J. Solution. Chem. 24 (1995) 551–563, https://doi.org/10.1007/BF00973206.
[126] W. Yan, Y. Xu, S. Han, Activity coefficients of sodium chloride in methanol-water mixed solvents at 298.15 K, Acta Chimica Sinica 52 (1994) 937–946 (in Chinese).
[127] J.T. Safarov, Study of thermodynamic properties of binary solutions of lithium bromide or lithium chloride with methanol, Fluid. Phase Equilib. 236 (2005) 87–95, https://doi.org/10.1016/j.fluid.2005.07.002.
[128] J. Barthel, G. Lauermann, R. Neueder, Vapor pressure measurements on non-aqueous electrolyte solutions. Part 2. Tetraalkylammonium salts in methanol. Activity coefficients of various 1-1 electrolytes at high concentrations, J. Solution. Chem. 15 (1986) 851–867, https://doi.org/10.1007/BF00646092.
[129] J.T. Safarov, Vapor pressures of lithium bromide or lithium chloride and ethanol solutions, Fluid. Phase Equilib. 243 (2006) 38–44, https://doi.org/10.1016/j.fluid.2006.02.012.
[130] K. Nasirzadeh, R. Neueder, W. Kunz, Vapor Pressures, Osmotic and Activity Coefficients of Electrolytes in Protic Solvents at Different Temperatures. 2. Lithium Bromide in Ethanol, J Solution Chem. 33 (2004) 1429–1446, https://doi.org/10.1007/s10953-004-1057-9.
[131] J. Barthel, G. Lauermann, Vapor pressure measurements on non-aqueous electrolyte solutions. Part 3: Solutions of sodium lodide in ethanol, 2-propanol, and acetonitrile, J. Solution. Chem. 15 (1986) 869–877, https://doi.org/10.1007/BF00646093.
[132] M.T. Zafarani-Moattar, K. Nasirzade, Osmotic Coefficient of Methanol + LiCl, + LiBr, and + LiCH $_3$ COO at 25°C, J. Chem. Eng. Data. 43 (1998) 215–219, https://doi.org/10.1021/je970193e.
[133] P.A. Skabichevskii, Osmotic coefficients of lithium chloride and bromide solutions in methanol, RUSSIAN JOURNAL OF PHYSICAL CHEMISTRY 43 (1969), 1432-+.
[134] R.R. Kolhapurkar, P.K. Patil, D.H. Dagade, K.J. Patil, Studies of Thermodynamic Properties of Binary and Ternary Methanolic Solutions Containing KBr and 18-Crown-6 at 298.15 K, J. Solution. Chem. 35 (2006) 1357–1376, https://doi.org/10.1007/s10953-006-9066-5.
[135] O.D. Bonner, The colligative properties of certain electrolytes and non-electrolytes in methanol, J. Solution. Chem. 16 (1987) 307–314, https://doi.org/10.1007/BF00646122.
[136] K. Nasirzadeh, A. Salabat, Isopiestic determination of osmotic coefficients and evaluation of vapor pressures for solutions of sodium bromide and sodium thiocyanate in methanal at 25°C, J. Mol. Liq. 106 (2003) 1–14, https://doi.org/10.1016/S0167-7322(03)00016-3.
[137] Z.C. Wang, X.Y. Li, Y.H. Liu, Isopiestic studies on (methanol + sodium bromide + ammonium bromide) at the temperature 298.15 K: comparison with the partial ideal solution model, The Journal of Chemical Thermodynamics 30 (1998) 709–712, https://doi.org/10.1006/jcht.1997.0335.
[138] K. Bräuer, H. Strehlow, Die Normalpotentiale des Kaliums und Rubidiums in Methanol, Zeitschrift für Physikalische Chemie 17 (1958) 346–349, https://doi.org/10.1524/zpch.1958.17.5_6.346 (in German).
[139] N.A. Izmailov, E.F. Ivanova, Thermodynamic properties of electrolyte in nonaqueous solutions. II. Research of solutions of NaBr, NaI and KBr in ethanol

and NaI in n-butanol and change of energy of ions at change of solvents, Zhurnal Fizicheskoi Khimii 29 (1955) 1614–1623 (in Russian).
[140] S.J. Kim, J.H. Kim, K.S. Choi, The behavior of electrolytes in nonaqueous solutions (IV). Relative viscosities and osmotic coefficients of alkaline metal iodies, Journal of the Korean Chemical Society 28 (1984) 349–354 (in Korean).
[141] U. Westhaus, DETHERM, (2019).
[142] S. Reiser, M. Horsch, H. Hasse, Density of Methanolic Alkali Halide Salt Solutions by Experiment and Molecular Simulation, J. Chem. Eng. Data. 60 (2015) 1614–1628, https://doi.org/10.1021/je5009944.
[143] G. Jones, H.J. Fornwalt, The Viscosity of Solutions of Salts in Methanol, J. Am. Chem. Soc. 57 (1935) 2041–2045, https://doi.org/10.1021/ja01314a007.
[144] J.I. Lankford, W.T. Holladay, C.M. Criss, Isentropic compressibilities of univalent electrolytes in methanol at 25°C, J. Solut. Chem. 13 (1984) 699–720, https://doi.org/10.1007/BF00649010.